جامعة بيرزيت
BIRZEIT UNIVERSITY

Faculty of Graduate Studies

The Reaction of Zinc(II) Piroxicam Complexes with Nitrogen Based Ligands. Synthesis, Characterization and Biological Activity of the New Complexes.

تفاعل معقد الزنك ثنائي الشحنة مع البايروكسيكام والقواعد النيتروجينية المختلفة. التحضير، التركيب والخصائص البيولوجية للمعقدات الجديدة.

This thesis was submitted in partial fulfillment of the requirements for the Master's Degree in in applied chemistry from the Faculty of Graduate Studies at Birzeit University, Ramallah, Palestine

Sabreen Basim Tawafsha

Under Supervision of **Prof. Hijazi Abu Ali**

Feb., 2021

The Reaction of Zinc(II) Piroxicam Complexes with Nitrogen Based Ligands. Synthesis, Characterization and Biological Activity of the New Complexes.

By

Sabreen Basim Tawafsha

This thesis was defended successfully on 01/02/2021 and approved by:

Committee Members Signature

Prof. Hijazi Abu Ali

Supervisor

Department of Chemistry, Birzeit University

Dr. Arwa Abu Khweek

Member of thesis committee

Department of Biology and Biochemistry, Birzeit University

Dr. Wadie Sultan

Member of thesis committee

Department of Chemistry, Al-Quds University

Acknowledgements

First of all, thanks to Allah Almighty for his blessing with good opportunities and gorgeous people.

I would like to express my gratitude to my supportive supervisor Prof. Hijazi Abu Ali, who has taught me to carry out this research and kindly supported me throughout my research work to complete it successfully.

To my master's thesis committee, Dr. Arwa Abu Kweek, and Dr. Wadie Sultan, their efforts in reading and discussing work is highly appreciated.

I would like to thank all Chemistry Department members especially Dr. Ibrahim Shalash, and Mr. Azmi Dudin for their kind help throughout my research period, and many thanks for Mr. Assem Mubark for his continuing support. I would also like to thank Mr. Munther Matani and Mr. Rateb Mohammad at Biology Department for their help and patience in performing the biological activity applications.

Especial thanks to Al-Quds Pharmaceutical Company for their generous donation of the piroxicam compound.

To my parents, Basim and Nuzha, I am extremely grateful for their love and caring during my life. This work for them with much of love and gratitude.

To my inspirational, beloved husband, Majd Ishtaya, all words of thanks and praise do not fulfill his right, I am thankful for his support, patience, and love.

I am extending my heartfelt thanks to all of my family, my lovely sister (Yasmeen), my brothers (Mohammed, and Hamad), Bilal Shalash, Shama Olwan, Bilal Ishtaya, and Wesam Birawi for their support.

I would like to thank my friends, Laila Khalil, Mayes Majadleh, Fatima Hamdan, and Istabraq Yahia for their support.

To my first place, my first step, all my memories, the past, the present and the future, Birzeit University, all of love and thanks.

Birzeit, Feb. 2021

Sabreen Basim Tawafsha

Contents

List of Figures

List of Tables

List of Schemes

Abbreviations

Pir	Piroxicam
1,10-phen	1,10-phenethroline
2,2'-bipy	2,2'-bipyrdine
2-ampy	2-aminopyridine
2-picolyl	2-picolylamine
IR	Infrared
UV-Vis	Ultraviolet-Visible
^{1}H-NMR	Proton Nuclear Magnetic Resonance
NMR multiplicities	s = Singlet d = Doublet t = Triplet m = Multiplet
IZD	Inhibition Zone Diameter
DW	Distilled Water
NSAIDs	Non-steroidal anti-inflammatory drugs
OM	Outer membrane
BNPP	bis-(4-nitrophenyl) phosphate
G	Gentamicin
E	Erythromycin
Pyr	Pyridyl
G^{+}	Gam-positive bacteria
G^{-}	Gam-negative bacteria

Abstract

New mononuclear Zn(II) complexes derived from piroxicam and different nitrogen-based ligands [Zn(Pir)(1,10-phen)$_2$] (**1**), [Zn(Pir)(2,2'-bipy)] (**2**), [Zn(Pir)(2-ampy)$_2$] (**3**), and [Zn(Pir)$_2$(2-picolyl)$_2$] (**4**) have been synthesized and characterized by IR, UV-Vis, ^{1}H-NMR spectroscopy, and other physical properties.

In vitro anti-bacterial activity of the new zinc complexes (**1-4**) was evaluated using agar diffusion method against five Gam-positive bacteria (*Staphylococcus aureus, Micrococcus luteus, Bacillus subtilis, Enterococcus faecalis and Staphylococcus epidermidis*) and four Gram-negative bacteria (*Pseudomonas aeruginosa, Klebsiella pneumonia, Escherichia coli, Proteus mirabilis*). According to the Gram-negative bacteria, complexes **3** and **4** did not show any sensitivity toward Gram-negative bacteria. Complexes **1** and **2** showed anti-bacterial activity against *K. pneumonia, E. coli, P. mirabilis* with inhibition zone diameter (IZD) values between 20.7-30.3 mm, 9.3-19.0 mm, respectively. The highest IZD value, 30.3 mm, was for complex **1** against *P. mirabilis*.

In contrast, most complexes showed anti-bacterial activity against Gam-positive bacteria. Complexes **2** and **3** showed anti-bacterial activity against *S. aureus*, *B. subtilis*, and *S. epidermidis* with IZD values between 13.6-24.3 mm, and 15.3-22.7 mm, respectively. Complex **4** showed anti-bacterial activity against *S. aureus* and *S. epidermidis* with IZD values of 22.0 mm, and 25.3 mm, respectively. Complex **1** only showed anti-bacterial activity against *M. luteus* according to Gram-positive bacteria with IZD value of 25.0 mm. In addition, the enzymatic activity of these complexes was tested to measure the rate of BNPP hydrolysis at different concentrations, pH, and temperatures. The rate of zinc complexes was arranged as follows: **3** (40 ºC) > **4** (25 ºC) > **2** (37 ºC) > **1** (37 ºC).

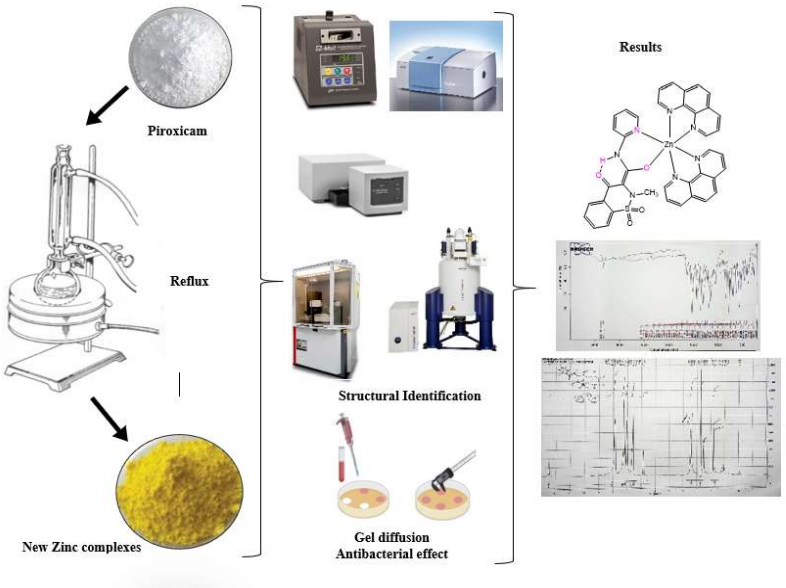

ملخص بالعربية

معقدات زنك جديدة أحادية النواة مشتقة من البايروكسيكام وقواعد نيتروجينية مختلفة $[Zn(Pir)(1,10\text{-phen})_2]$ (**1**)، $[Zn(Pir)(2,2'\text{-bipy})]$ (**2**)، $[Zn(Pir)(2\text{-ampy})_2]$ (**3**)، و $[Zn(Pir)_2(2\text{-picolyl})_2]$ (**4**) تم تحضيرها وتشخيصها باستخدام مطياف الأشعة تحت الحمراء، مطياف الأشعة فوق البنفسجية والمرئية، جهاز الرنين المغناطيسي، وخصائص فيزيائية أخرى.

في المختبر، النشاط المضاد للبكتيريا لمعقدات الزنك الجديدة (**1-4**) تم تقييمه باستخدام طريقة الانتشار في الآجار ضد خمسة أنواع من البكتيريا موجبة الغرام (*Staphylococcus aureus, Micrococcus luteus, Bacillus subtilis, Enterococcus faecalis and Staphylococcus epidermidis*) وأربعة أنواع من البكتيريا سلبية الجرام (*Pseudomonas aeruginosa, Klebsiella pneumonia, Escherichia coli, Proteus mirabilis*). بالنسبة للبكتيريا سلبية الجرام، المعقدان **3** و**4** لم يظهرا أي حساسية اتجاه هذه السلالات البكتيرية المختبرة. المعقدان **1** و**2** أظهر نشاطًا مضادًا للبكتيريا ضد *K. pneumonia, E. coli, P. mirabilis* بقيم قطر منطقة التثبيط بين 9.3-19.0 mm, 20.7-30.3mm, على التوالي. أعلى قيمة لقطر منطقة التثبيط كانت للمعقد **1** ضد *P. mirabilis* وتساوي 30.3 mm.

في المقابل، أكثر المعقدات أظهرت نشاطًا مضادًا للبكتيريا ضد البكتيريا موجبة الجرام. المعقدان **2** و**3** أظهرا نشاطًا مضادًا للبكتيريا ضد *S. aureus*, *B. subtilis*, and *S. epidermidis*

بقيم قطر منطقة التثبيط بينmm 13.6-24.3، 15.3-22.7 mm على التوالي. معقد **4** أظهر نشاطًا مضادًا للبكتيريا ضد *S. aureus* and *S. epidermidis* بقطر منطقة التثبيط يساوي 22.0 mm، 25.3 mm، على التوالي. معقد **1** الوحيد الذي أظهر نشاطًا مضادًا للبكتيريا ضد *M. luteus* من البكتيريا موجبة الجرام بقيمة قطر منطقة التثبيط تساوي 25.0 mm. بالإضافة لذلك، أُختبر النشاط الإنزيمي لهذه المعقدات لقياس سرعة تحلل BNPP عند تراكيز وقيم pH ودرجات حرارة مختلفة. سرعة معقدات الزنك ترتبت كما يلي: (40 ºC) **3** > (25 ºC) **4** > **2** (37 ºC) < (37 ºC) **1**.

1. Introduction

1.1 General overview

Metal elements are considered as building blocks of life which are required to maintain the growth and development of all biological systems and ecosystems in the planet[1]. Until now, 118 elements were found, 92 of them occur naturally. Nevertheless, about 26 elements are found in living organisms, and only six of them present the weight of most living organisms as shown in Figure 1[2]. In human body, atoms of these six elements called "organogens" (O, H, C, N, P, S) due to their special role in forming tissues, organs, and large molecules such as lipids, proteins, carbohydrates, nucleic acid etc. The remaining twenty elements are essential for life, and some of them such as iron and zinc are found in the human body in small amounts, called “trace elements” and their daily requirement is <100 ppm, Table 1[3,4,5,6,7].

Figure 1: The elemental composition of the human body by mass[8].

Table 1: Dietary reference intakes for essential trace elements (units/day) [7].

Life stage	Cr (µg)	Cu (mg)	F⁻ (mg)	I (mg)	Fe (mg)	Mn (mg)	Mo (mg)	Se (µg)	Zn (mg)
Children									
0–6 mo	0.2[a]	0.20[a]	0.01[a] {0.7}	0.11[a]	0.27[a] {40}	0.003[a]	0.002[a]	15[a] {45}	2[a] {4}
7–12 mo	5.5[a]	0.22[a]	0.5[a] {0.9}	0.13[a]	11[b] {40}	0.6[a]	0.003[a]	20[a] {60}	3[b] {5}
1–3 yr	11[a]	0.34[b] {1}	0.7[a] {1.3}	0.09[b] {0.2}	7[b] {40}	1.2[a] {2}	0.017[b] {0.3}	20[b] {90}	3[b] {7}
4–8 yr	15[a]	0.44[b] {3}	1[a] {2.2}	0.09[b] {0.3}	10[b] {40}	1.5[a] {3}	0.022[b] {0.6}	30[b] {150}	5[b] {12}
9–13 yr	25[a] (m) 21[a] (f)	0.7[b] {5}	2[a] {10}	0.12[b] {0.6}	8[b] {40}	1.9[a] (m) 1.6[a] (f) {6}	0.034[b] {1.1}	40[b] {280}	8[b] {23}
14–18 yr	35[a] (m) 24[a] (f)	0.89[b] {8}	3[a] {10}	0.15[b] {0.9}	11[b] (m) 15[b] (f) {45}	2.2[a] (m) 1.6[a] (f) {9}	0.043[b] {1.7}	55[b] {400}	11[b] (m) 9[b] (f) {34}
Adults									
19–50 yr	35[a] (m) 25[a] (f)	0.9[b] {10}	4[a] (m) 3[a] (f) {10}	0.15[b] {1.1}	8[b] (m) 18[b] (f) {45}	2.3[a] (m) 1.8[a] (f) {11}	0.045[b] {2}	55[b] {400}	11[b] (m) 8[b] (f) {40}
51+ yr	30[a] (m) 20[a] (f)				8[b] {45}				
Pregnancy									
14–18 yr	29[a]	1[b] {8}	3[a] {10}	0.22[b] {0.9}	27[b] {45}	2[a] {9}	0.05[b] {1.7}	60[b] {400}	12[b] {34}
19–50 yr	30[a]	1[b] {10}		0.22[b] {1.1}		2[a] {11}	0.05[b] {2}		11[b] {40}
Lactation									
14–18 yr	44[a]	1.3[b] {8}	3[a] {10}	0.29[b] {0.9}	10[b] {45}	2.6[a] {9}	0.05[b] {1.7}	70[b] {400}	13[b] {34}
19–50 yr	45[a]	1.3[b] {10}		0.29[b] {1.1}	9[b] {45}	2.6[a] {11}	0.05[b] {2}		12[b] {40}

a = Average Intake (AI) value

b = Recommended dietary allowance (RDA) value

{..} = Tolerable upper intake level (UL) value

All living systems need the availability of following elements H, C, N, O, Mg, P, S, Ca, Na, K, Cl, Mn, Fe, Cu, Zn, and Mo. The first eleven elements are the major elements, and they are present in large quantities. The remainder and iron are trace elements[9], Figure 2.

Trace elements play specific role in the body. The permanent presence of an element in the body and its association with enzymes, blood, proteins, nerves, and tissues is important to help regulating and activating vital functions at all stages of growth of the organism. When their concentration level is below certain limit of growth of the organism and when which will lead to the reduction in an important function; it is then considered an essential trace element[4,7].

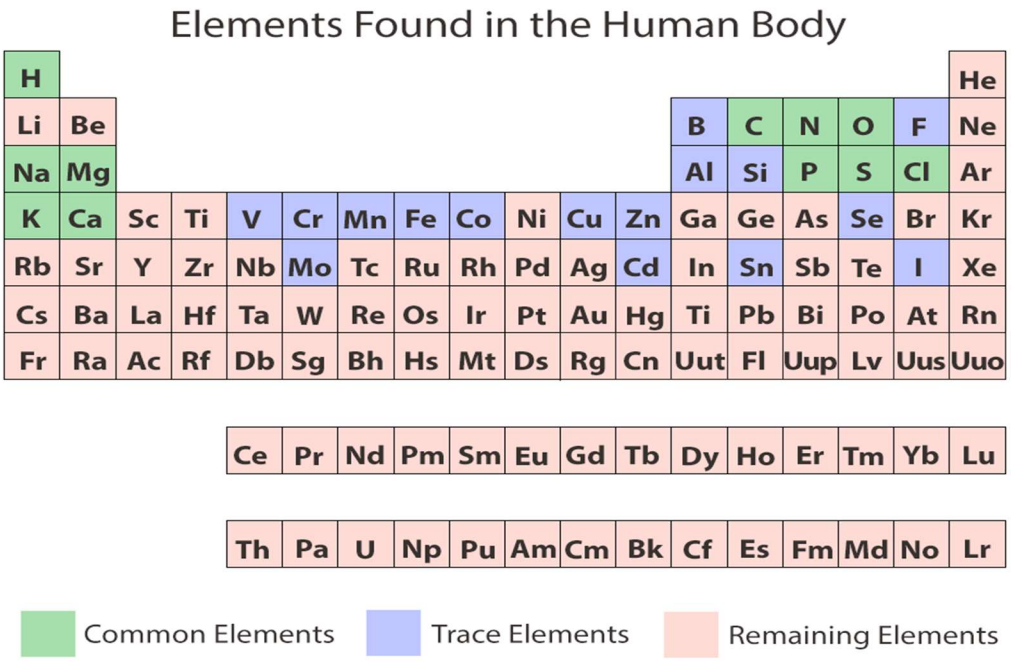

Figure 2: Elements found in the human body[10].

For each "essential" trace element, there is a range of quantity required by the body, which is adequate to maintain optimal functions, Figure 3[11]. Therefore, lower or higher concentration of these elements can be toxic for the body and affect the biological functions which may produce diseases, such as various types of cancer[6,12].

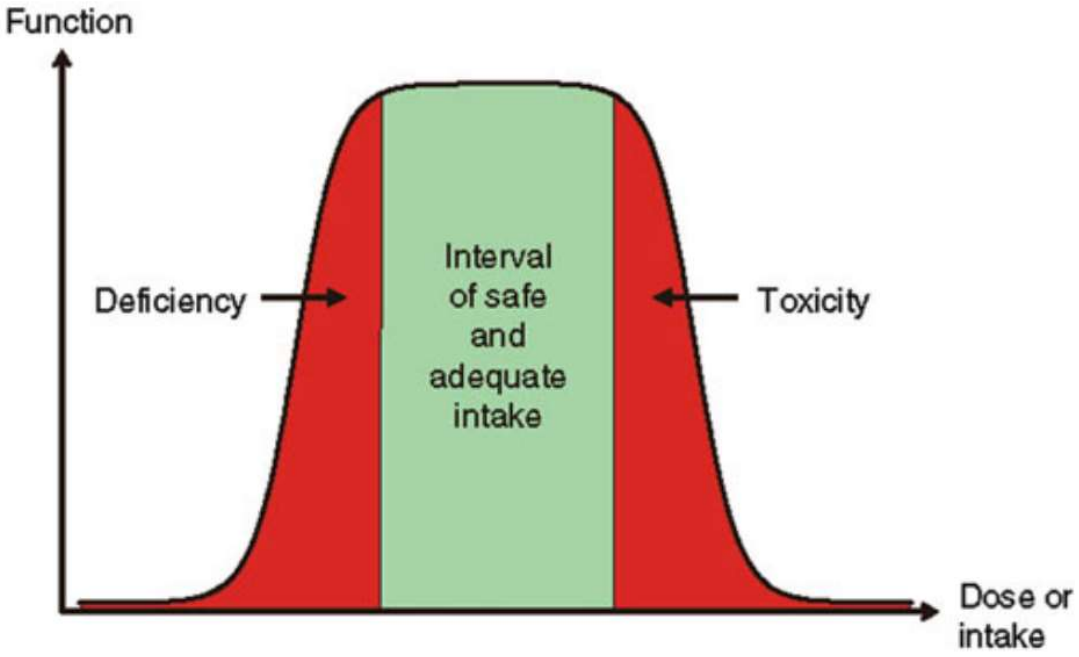

Figure 3: Dose-response of essential trace elements[13].

1.2 Zinc

1.2.1 Significance of zinc in biological system

Zinc is an essential trace element required by all living organisms, and is a vital micronutrient for human health[14,15]. It is considered the second most available trace element after iron in the human body[16]. Adult human's body contains 2.3 g of zinc which are distributed throughout the organs of the body as shown in Figure 4[17]. It cannot be stored in the body, so regular intake of zinc is a must to maintain a constant content of zinc in the body

for functioning[18]. The recommended dietary allowance (RDA) of zinc for adult men is 11 mg/d and 8 mg/d for women as previously shown in Table 1.

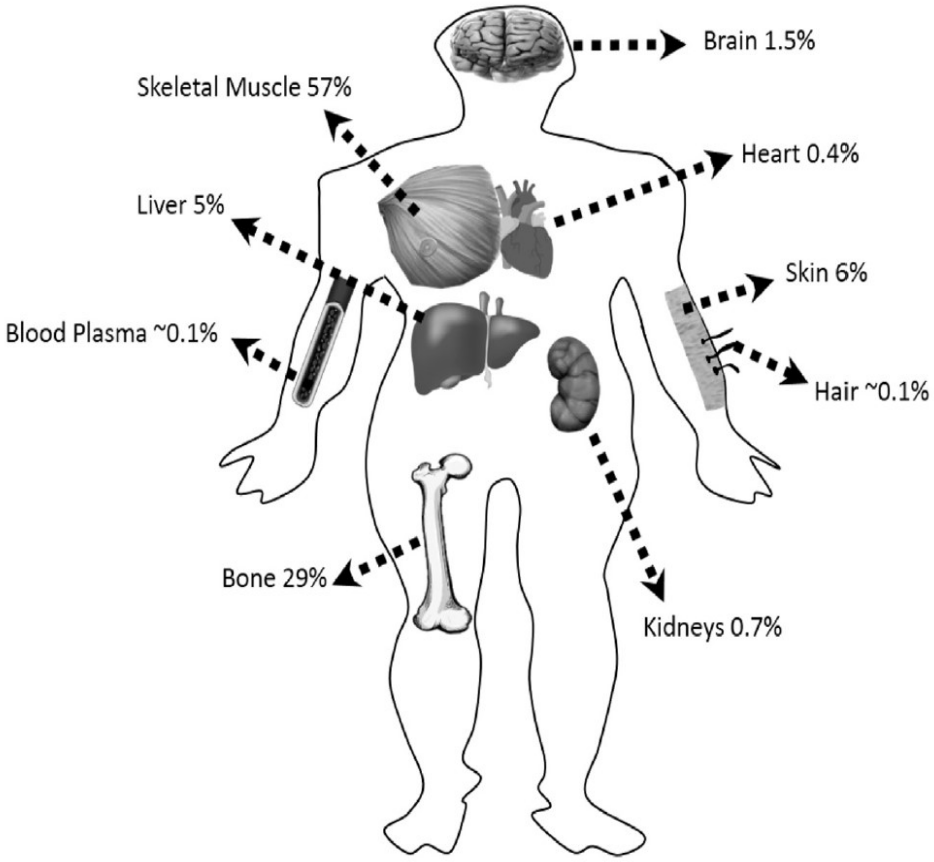

Figure 4: Zinc distribution in the body[19].

There are different sources of zinc such as red meats and other animal proteins. Other sources of Zn are seafood, dairy foods, cereals, and nuts, Table 2[20].

Table 2: Dietary zinc sources in selected foods [21].

Food	Serving size	Zinc content(mg)
Beef (ground beef)	¼ pound raw meat	4.3
Poultry (breast, bone)	½ breast (98 g)	1.0
Poultry (thigh, bone removed)	1 thigh	1.5
Oysters	3 oz cooked	4.2
Crab	3 oz cooked	3.2
Milk (2% low fat)	1 cup	1.0
Yogurt (low fat)	1 cup	1.8
Sunflower seeds (roasted)	1 oz dry	1.5
Whole grains	1 slice of bread	1.0
Legumes (navy beans)	1 cup	7.6

In the body, the binding of zinc makes its absorption from the animal source better than the vegetarian source. The existence of phytates in plants inhibit the Zn absorption due to its chelating with Zn. But in meat for an

example, zinc is present in high quantity and bound to ligands which simplify its absorption[22,23].

The biological functions of zinc in the body can be divided into three categories: catalytic, structural, and regulatory[24]. In the catalytic role, zinc ion plays as a co-factor for the synthesis of over than 300 enzymes, appears in all enzyme classes, and acts as a core ion of their reaction center, Table 3[25,26].

Table 3: Zinc metal metalloenzymes in the six enzyme classes[27].

Class	Enzyme
Oxidoreductase	Alcohol dehydrogenase, Superoxide dismutase, Malic dehydrogenase, Lactic dehydrogenase
Transferase	RNA polymerase, DNA polymerase, Reverse transcriptase
Hydrolase	Alkaline phosphatase, Carboxypeptidase A, B, Collagenase
Lyase	Carbonic anhydrase
Isomerase	Phosphomannose isomerase
Ligase	tRNA synthetase

In the structural role, zinc plays a role in folding the different proteins in our body by the coordination of one or more zinc ions (Zn) to produce biological active molecules such as zinc finger proteins[28]. Zinc finger plays an important role in recognition of DNA during replication and is essential for the function of some transcription factors[29]. And as a structural role, zinc gives a structural function for some enzymes[28].

Finally, the presence of zinc in the body affects gene expression as a regulatory influence[30]. Zn also plays an important role in the regulation of the immune system; it regulates the growth of thymic T cells, production of inflammatory cytokine, and neutrophils to kill microorganisms. In addition, the regulation of zinc appears in metallothionein effective anti-oxidant function[19, 26].

Zinc also have multi functions and needed for growth of muscles, hair, nails, cell division wound healing; in addition, it helps in the treatment of some diseases such as cancer and heart diseases[19, 27].

Based on the above, many organs in the body will be affected if zinc deficiency occurs. Deficiency usually caused when intake of zinc is less than RDA or deficiency in the body such as anemia. There are some

symptoms that indicate zinc deficiency like diarrhea, alopecia, and defects in reproductive, also the immune system will be affected[27].

1.2.2 Zinc as an element

Zinc (Zn^{+2}) a divalent cation, has an atomic number of 30 that exist in group 12 and period 4 of the Periodic Table[31]. The abundance of zinc in earth's crust is about 0.0078%, so it is the 24th most abundant element and it has five stable isotopes ^{64}Zn (48.6%), ^{66}Zn (27.9%), ^{67}Zn (4.1%), ^{68}Zn (18.8%), and ^{70}Zn (0.6%). It has a shiny bluish-white color[27,32].

The electron configuration of Zn^{+2} is [Ar]$3d^{10}$, with filled *d* shell gives some features such as its flexibility to adopt four, five, and six coordination geometries, and in any of these geometries it has no ligand field stabilization energy when coordinated to ligands. Zn^{+2} is considered a borderline Lewis acid in terms of hard soft acid base concept (HSAB), so Zn^{+2} can interact with different donor ligands including sulfur, oxygen, or nitrogen in human body from cysteine, glutamate, and histidine, respectively. Finally, zinc does not participate in redox reactions[33].

1.3 Chelating Agents

The chemical compounds with two or more donor atoms can bind to metal ions to form a metal chelate with one or more rings, these compounds are called chelating agents or chelates. In general, most of metals react with O-, S-, and N-containing ligands (donor heteroatoms), because of the lone pair/pairs of electrons which they have. These ligands can be classified as bidentate, tridentate, tetradentate and so higher dentate, Figure 5[34,35,36].

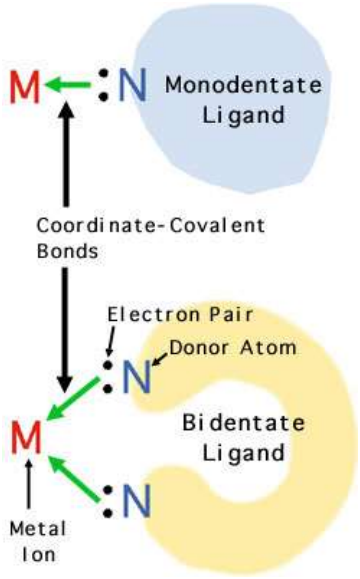

Figure 5: The monodentate and bidentate ligands along with donor atom and metal[37].

Due to their ability to complex metals, chelating agents have been used in several applications such as corrosion inhibitors, textile and paper

production, inhibition of the growth of microorganisms, wastes and effluents treatment, agriculture, metal electroplating, tanning, photography, food products, pharmaceuticals, and cosmetics. And based on the process type, the chelates act in two different processes: removal of metals which can affect the efficiency of the process, or to avoid metal precipitation and maintain a necessary amount that helps to continue the process[38].

Bioactive nitrogen base compounds are the most important class of ligands in coordination chemistry like 2,9-dimethyl-1,10-phenanthroline, quinoline, 2-aminopyridine, 2-amino-6-picoline, 1,0-phenethroline and 2-methylaminopyrdine shown in Figure 6 play a significant role in coordination chemistry due to their new diagnostic and therapeutic agents.

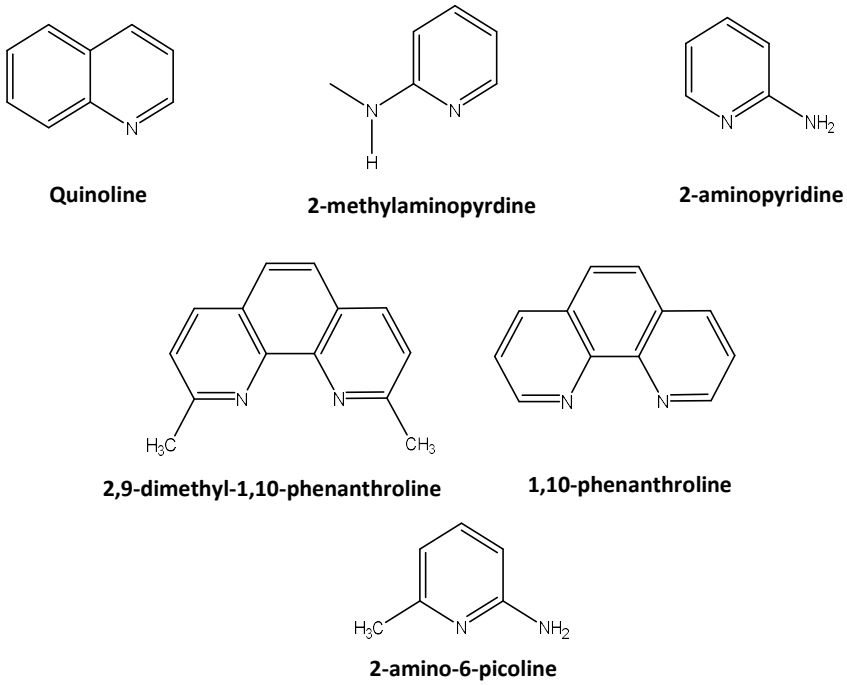

Figure 6: Chemical structures of some bioactive nitrogen compounds.

These ligands are received much attention because of their biological activity which includes anti-inflammatory, antitumoral, antifungal, anti-microbial, anti-viral activity, and anti-carcinogenic properties[39,40,41,42,43,44].

The interaction of ligands with metal ions afforded many active complexes in various geometries[45]. Chelating ligands have different mode of interaction to metal ions; we find that each ligand has a different mode. For example, 1,10-phenanthroline behave as bidentate ligand towards

metal ions as reported and shown in Figure 7 whereas the chelating mode of quinoline is monodentate[46,47,48].

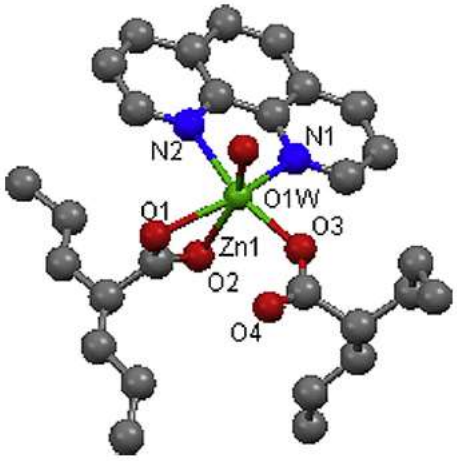

Figure 7: The molecular structure of $[Zn(valp)_2(1,10\text{-phen})H_2O]$ complex[46].

1.4 Metal oxicams complexes

Oxicam series is a class of nonsteroidal anti-inflammatory drugs (NSAIDs) and belong to the enolic acid class of 4-hydroxy-1,2 benzothiazine carboxamides according to its structure. In addition, oxicams are considered as the NSAIDs which have no carboxylic acid (carboxylate-lacking NSAIDs) such as piroxicam, tenoxicam, meloxicam, lornoxicam and isoxicam, Figure 8[49]. These oxicams are the most studied species of the series due to their activity and strong ability to chelate metal ions in biomedical chemistry[50].

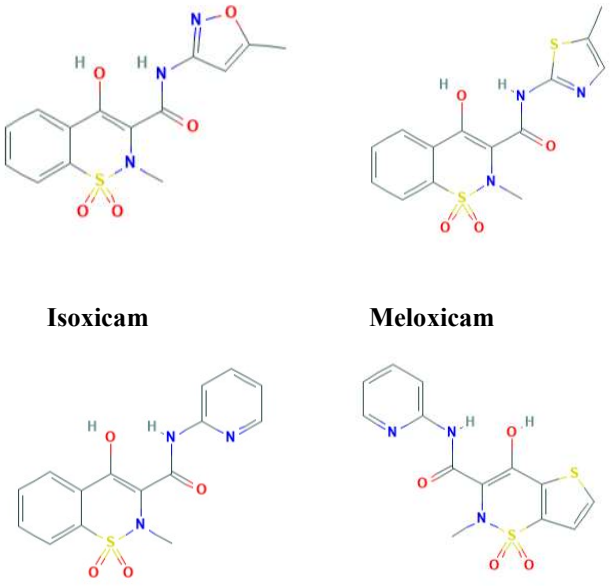

Isoxicam **Meloxicam**

Piroxicam **Tenoxicam**

Figure 8: Chemical structures of some nonsteroidal carboxylate-lacking anti-inflammatory drugs[51].

Many previous works and studies showed different coordination modes toward metal ions of oxicam drugs. For instance, the coordination of tenoxicam (H_2ten) to Cu(II) was through the amide oxygen and pyridyl nitrogen atom in $[Cu(Hten)_2(py)_2]\cdot$ EtOH complex[52].

In the synthesis of metal complexes, the solubility of each reactant in the reaction mixture is important. All oxicams are insoluble in water, even so, the synthesis of oxicams occur in hot EtOH, hot MeOH, DMSO, or benzene[50].

There are significant attempts to replace a lot of parent drugs with their transition metal complexes which were synthesized and tested for their various activities and showed good impacts[53].

1.5 Piroxicam

Piroxicam, (2H-1,2-benzothiazine-3-carboxamide-4-hydroxy-2-methyl-N-2-pyridinyl-1,1-dioxide), Figure 9, with a molecular formula $C_{15}H_{13}N_3O_4S$, is an enolic benzothiazine and a potent member of non-steroidal anti-inflammatory drug of the oxicam series[54,55,56].

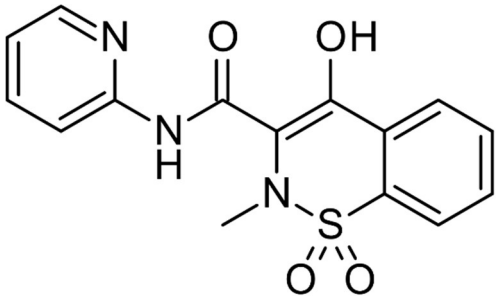

Figure 9: Chemical structure of piroxicam.

This drug has an anti-inflammatory effect and act as analgesic, hyperglycemic, antihypertensive, and antipyretic agent. These effects are produced after injury or disease by inhibiting one or both cyclooxygenases

(COX) isoenzymes, where COX is the key enzyme in the synthesis of prostaglandin, their inhibition decrease the prostaglandin production[54,57,58]. Piroxicam is a crystalline solid and soluble in most organic solvents and diluted acids. It is effective as an oral treatment of musculoskeletal pains, including osteoarthritis and rheumatoid arthritis. The daily dose to achieve a therapeutic effect of those pains is 20 mg as a singlet and considered as a low dose because of its long half-life time (40 hours)[55,59,].

As any drug, though the effective therapy of piroxicam, it has some adverse effects such as gastrointestinal ulceration and renal disorder[55].

1.5.1 Piroxicam metal complexes

Many previous studies showed the enhancement of metal complexes of drugs activity due to the beneficial effects of ligands and metal[60,61]. NSAIDs as mentioned previously have an important role which classified them as the most frequently used medicinal drugs and their activities were enhanced upon metal complexation. Piroxicam is a one example of such compounds[62,63].

Piroxicam has stable conformational isomers (rotamers) with *EZE* and *ZZZ*, Scheme 1. It is known that piroxicam react either as a monodentate

ligand via the pyridyl nitrogen atom, or as a bidentate chelating ligand via the pyridyl nitrogen atom and the amide oxygen atom, or as a tridentate ligand through the enolic oxygen, nitrogen atoms of the pyridyl and the amide groups[62].

Scheme 1: Possible conformational rotamers of piroxicam.

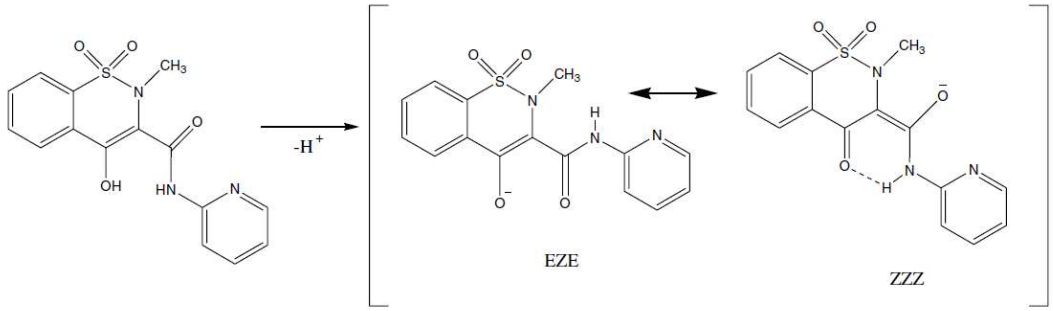

The chelation behavior of piroxicam with metals varies from metal to another. It reacts as a monodentate ligand towards Pt(II), as a bidentate chelating towards Cu(II), Cd (II), Fe(II), Co(II), Ni(II) and Zn(II) metal cations as shown in Figure 10, and as tridentate in the Sn(IV) complex[58].

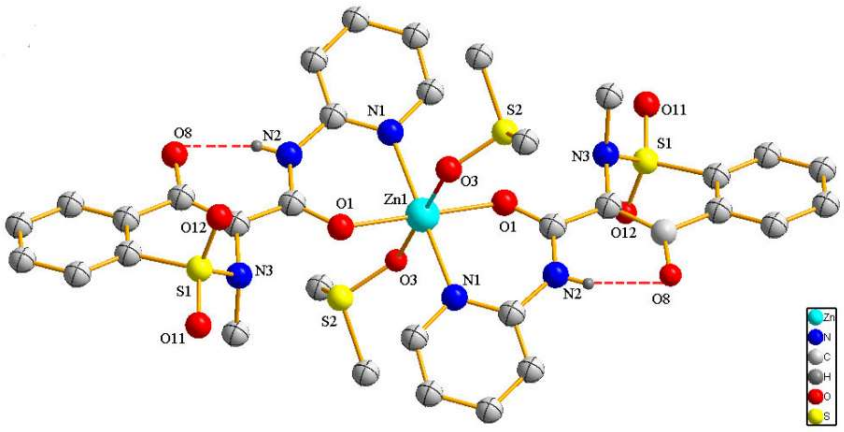

Figure 10: Molecular structure of the trans-$[Zn(Pir)_2(DMSO)_2]$ complex[64].

Various experimental results showed enhanced drugs activity of the metal complexes compared to their free ligands and their metal salt precursors, trans $[Zn(Pir)_2(DMSO)_2]$ complex as an example showed enhanced activity when it was applied in the investigation of the cytotoxicity on human myelogenous leukemia cell line[64].

Based on the encouraging results of previously reported literature the present work will focus on the synthesis of Zn(II), piroxicam, and different nitrogen-based ligands complexes.

Each of the complex three components has significant roles, Zn(II) as an example, in addition to its biological activity in the body, it has an effect

in bacterial inhibition. It showed an inhibitory action on the growth of different types of bacteria i.e., *Escherichia coli*, *Entrococcus faecalis*, *Staphylococcus aureus*, *Staphylococcus epidermidis*, and *Pseudomonas aeruginosa*[46].

1.6 Bis-(4-nitrophenyl) phosphate hydrolysis

The importance of phosphodiester bonds is derived from its role in the formation of the backbones of RNA and DNA as shown in Figure 11. Furthermore, other phosphate esters are involved in vital biological roles such as information storage (DNA/RNA) and processing, cellular signaling, regulation, and energy transduction (ATP)[65,66,67,68,69,70].

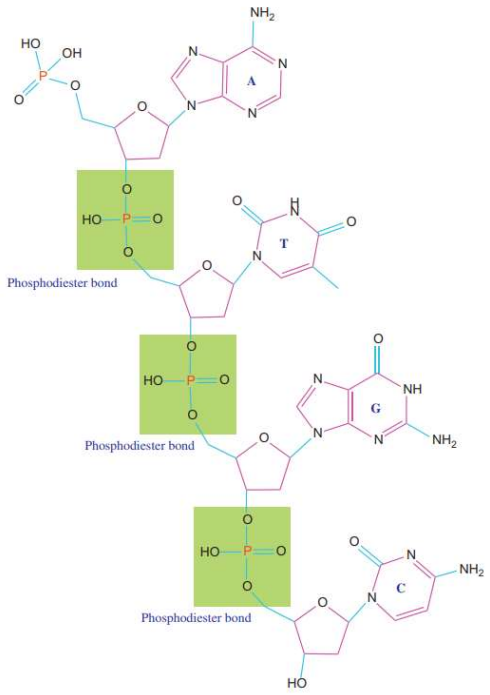

Figure 11: Phosphodiester bond linkage of DNA. Nucleotides in DNA are linked together by phosphodiester bonds[71].

These bonds are very stable and resistant towards hydrolytic processes due to the repulsion between the negatively charged backbone and potential nucleophiles[68,72].

In the absence of a catalyst, the half-life time of phosphate ester bonds hydrolysis is estimated to be about 100000 years and more for DNA and 4 years for RNA at neutral pH and 25 °C[67]. This stability gives the bonds their significance as the excellent systems for information storage and the

previously vital roles and others. Due to this stability, an enzymatic cleavage is required in biochemical fields. Phosphatases as a natural class of enzymes have one or more metal ions at the active sites that are responsible for hydrolyzing phosphodiester bonds[68]. On the other hand, bis-(4-nitrophenyl) phosphate (BNPP) compound can be used as a model to study the hydrolysis of the bonds, Figure 12.

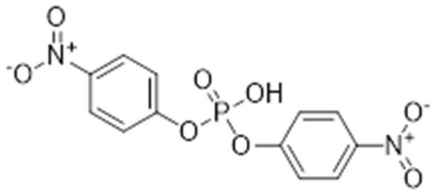

Figure 12: The chemical structure of BNPP ($C_{12}H_9N_2O_8P$).

In recent decades, the rapid hydrolytic cleavage of this molecule was studied by Ni(II), Cu(II), Ln(II), Zn(II) transition metal and different base ligands complexes as catalysts[72,73,74,75,76]. In addition to the biological applications, the hydrolysis of BNPP is vital in environmental, and industrial applications[48].

The roles of metal ions which act as Lewis acids based on activation of the phosphate group and nucleophilic H_2O molecule, and stabilization of the pentacoordinate phosphorus transition state by cooperative action in metalloenzymes[76,77].

Figure 13 shows the mechanism of BNPP catalytic hydrolysis by the main steps which are the interaction between metal complex and BNPP molecule to form the reaction intermediate by the coordination of oxygen atom on the P=O of BNPP with the metal complex. Then, release p-nitrophenol by the attack of the P atom in BNPP by metal hydroxide, which is the rate-determining step of the reaction. Also, the second p-nitrophenol and phosphoric acid are released rapidly, and the catalyst is regenerated in the BNPP hydrolysis cycle[48,78].

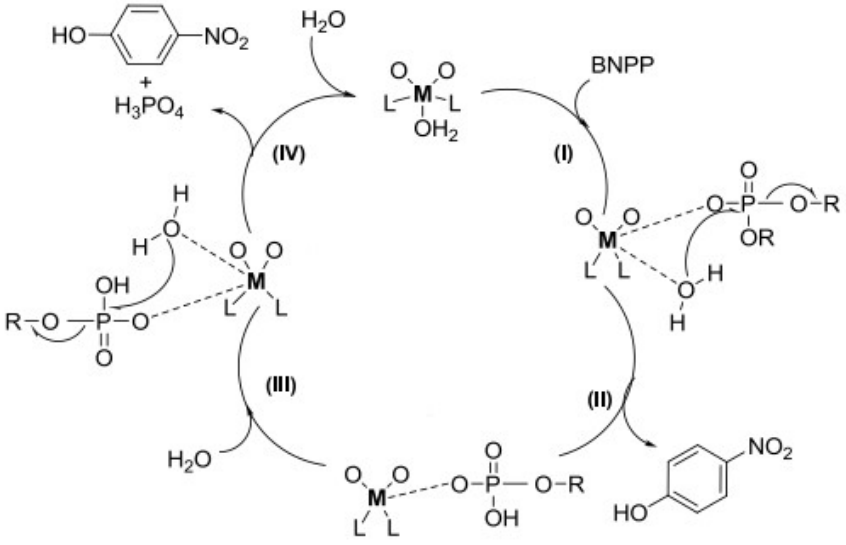

Figure 13: Reaction pathways for phosphate diester hydrolysis catalyzed by a metal ion.

1.7 Aim of the research

This research concerned with synthesis of new zinc complexes with different N-based ligands with the general formula $[Zn(Pir)_nL_m]$ (Pir = piroxicam, L = ligands such as 1,10-phenanthroline, 2,9-dimethyl-1,10-phenanthroline, quinoline, 2-amino-6-picoline, 2,2'-bibyridine, 2-aminopyrdine and 2-picolylamine, n = 1, 2, 3...; m = 1, 2, 3...).

The new complexes will be characterized by IR-spectroscopy, UV-spectroscopy and ^{1}HNMR spectroscopy.

The biological activity of these complexes and their parent ligands will be studied to evaluate the anti-bacterial activity and BNPP hydrolysis (bis-p-nitrophenyl phosphate) of the synthesized complexes.

2. Experimental

2.1 Materials

Piroxicam was donated by Al-Quds Pharmaceutical Company. All chemicals were of analytical grade. Reagents and solvents were high purity purchased from Merck, Sigma Aldrich, and Fluka chemical companies and were used without any further purification. All bacteria strains

(*Staphylococcus aureus, Micrococcus luteus, Bacillus subtilis, Enterococcus faecalis and Staphylococcus epidermidis*, *Pseudomonas aeruginosa, Klebsiella pneumonia, Escherichia coli, Proteus mirabilis*) were obtained from the Biology Department at Birzeit University.

2.2 Apparatus

To characterize the new Zn complexes, infrared spectra of solid samples were recorded with a Bruker TENSOR II Spectrometer in the 400-4000 cm^{-1} region. Kinetic measurements of BNPP hydrolysis and electronic spectra of the complexes and their parent compounds were carried out spectrophotometrically on Agilent 8453 UV-Vis spectrophotometer in solution of DMSO or MeOH, using quartz cell in the 200 to 800 nm spectral range. 300 MHz ^{1}H-NMR spectra were collected on a Varian Unity Spectrometer. Melting points were determined on an EZ-Melt melting point apparatus. Values of pH were detected by a Metrohm 827 pH meter.

2.3 Synthesis and characterization of zinc piroxicam complexes

2.3.1 Synthesis of [Zn(Pir)(1,10-phen)$_2$] (1)

5 ml of ethanolic solution of NaOH (0.3 mmol, 12.5 mg) was added dropwise with stirring to a solution of piroxicam (0.3 mmol, 99.4 mg) in ethanol (10 ml). To the resulting anionic piroxicam (Pir^-) solution was then added a hot ethanolic solution (60 °C, 10 ml) of $Zn(CH_3COO)_2 \cdot 2H_2O$ (0.15 mmol, 33.2 mg) and the mixture was stirred for 1 h. 1,10-Phen (0.3 mmol, 59.5 mg) was added and the mixture was then refluxed for 3 h. The solution was cooled to 0 °C and then was concentrated under vacuum to a minimum amount and the solution was filtered, the filtrate was kept at room temperature to give the desired yellow solid product.

[Zn(Pir)(1,10-phen)$_2$] (1). 74 % yield; m.p. = 172 °C (d); ^{1}H NMR (DMSO): δ (ppm) 2.73 (s, 3H, CH_3), 6.86 (d, 1H, CH, $^3J_{H\text{-}H}$ = 4.8 Hz), 7.60 (m, 4H, 4CH), 8.03 (d, 4H, 4CH, $^3J_{H\text{-}H}$ = 6.9 Hz), 8.18 (d, 4H, 4CH, $^3J_{H\text{-}H}$ = 3.0 Hz), 8.25 (d, 4H, 4CH, $^3J_{H\text{-}H}$ = 9 Hz), 8.88 (d, 4H, 4CH, $^3J_{H\text{-}H}$ = 6.0 Hz), 13.43 (s, 1H, NH). IR: ν/cm^{-1}; 3381, 2117, 1731, 1622, 1573, 1506,

1426, 1391, 1325, 1300, 1259, 1163, 1066, 846, 767, 724, 677, 627, 572, 546, 523, 405, 284; UV-Vis: λ_{max} (MeOH)/nm; 201, 229, , 360.

2.3.2 Synthesis of [Zn(Pir)(2,2'-bipy)] (2)

10 ml of ethanolic solution of NaOH (0.6 mmol, 25.3 mg) was added dropwise with stirring to a solution of piroxicam (0.6 mmol, 198.2 mg) in ethanol (20 ml). To the resulting anionic piroxicam (Pir^{-}) solution was then added a hot ethanolic solution (60 °C, 20 ml) of $Zn(CH_3COO)_2 \cdot 2H_2O$ (0.3 mmol, 66.2 mg) and the mixture was stirred for 1 h. 2,2-bipy (0.6 mmol, 93.3 mg) was added and the mixture was refluxed for 3 h. The solution was cooled to 0 °C and then was kept at room temperature, the solution was filtered, and the filtrate gives the desired yellow solid product.

[Zn(Pir)(2,2'-bipy)] (2). 64%, m.p. = 82-85 °C, ^{1}H NMR (DMSO): δ (ppm) 2.71 (s, 3H, CH_3), 6.89 (d, 1H, CH, $^3J_{H-H}$ = 6 Hz), 7.59 (m, 3H, 3CH), 7.66 (m, 3H, 3CH), 8.0 (d, 1H, CH, $^3J_{H-H}$ = 9 Hz), 8.48 (d, 1H, 2CH, $^3J_{H-H}$ = 3.6 Hz), 8.66 (d, 2H, 2CH, $^3J_{H-H}$ = 3 Hz), 13.49 (s, 1H, NH). IR: ν/cm^{-1}; 3384, 1731, 1621, 1600, 1572, 1505, 1473, 1428, 1391, 1329, 1300, 1258, 1157, 1065, 1018, 875, 837, 762, 737, 676, 652, 627, 572, 547, 523, 408. UV-Vis: λ_{max} (MeOH)/nm; 202, 235, 283, 357.

2.3.3 Synthesis of [Zn(Pir)(2-ampy)$_2$] (3)

10 ml of ethanolic solution of NaOH (0.6 mmol, 25 mg) was added dropwise with stirring to a solution of piroxicam (0.6 mmol, 198.4 mg) in ethanol (20 ml). To the resulting anionic piroxicam (Pir^-) solution was then added a hot ethanolic solution (60 °C, 20 ml) of $Zn(CH_3COO)_2 \cdot 2H_2O$ (0.3 mmol, 65.9 mg) and the mixture was stirred for 1 h. 2-ampy (1.2 mmol, 112.7 mg) was added and the mixture was refluxed for 3 h. The solution was cooled to 0 °C and then the solution was kept at room temperature and the filtrate gives the desired light-yellow solid product.

[Zn(Pir)$_2$(2-ampy)$_2$] (3). 71 % yield; m.p. = 51-53 °C; ^{1}H NMR (DMSO): δ (ppm) 2.71 (s, 3H, CH_3), 5.85 (s, 4H, $2NH_2$), 6.40 (m, 3H, 3CH), 6.86 (t, 2H, 2CH, $^3J_{H\text{-}H}$ = 12 Hz), 7.30 (t, 1H, CH, $^3J_{H\text{-}H}$ = 7.2 Hz), 7.63 (m, 3H, 3CH), 7.85 (d, 1H, CH, $^3J_{H\text{-}H}$ = 4.2 Hz), 7.99 (d, 1H, CH, $^3J_{H\text{-}H}$ = 7.5 Hz), 8.16 (d, 1H, 1CH, $^3J_{H\text{-}H}$ = 3.9 Hz), 13.39 (s, 1H, NH). IR: ν/cm^{-1}; 3483, 3378, 1743, 1620, 1568, 1507, 1482, 1441, 1378, 1332, 1265, 1229, 1153, 1117, 1061, 1038, 1002, 912, 858, 755, 682, 656, 631, 612, 571, 550, 519, 412. UV-Vis: λ_{max} (MeOH)/nm; 202, 295, 358.

2.3.4 Synthesis of [Zn(Pir)$_2$(2-picolyl)$_2$] (4)

5 ml of ethanolic solution of NaOH (0.3 mmol, 11.9 mg) was added dropwise with stirring to a solution of piroxicam (0.3 mmol, 99.1 mg) in ethanol (10 ml). To the resulting anionic piroxicam (Pir^-) solution was then added a hot ethanolic solution (60 ^oC, 10 ml) of $Zn(CH_3COO)_2 \cdot 2H_2O$ (0.15 mmol, 33.3 mg) and the mixture was stirred for 1 h. 2-picolyl (0.6 mmol, 64.6 mg) was added and the mixture was refluxed for 3 h. The solution was cooled to 0 ^oC and then was concentrated under vacuum to a minimum amount, the solution was filtered, and the filtrate was kept at room temperature to give the desired yellow solid product.

[Zn(Pir)$_2$(2-picolyl)$_2$] (4). 88 % yield; m.p. = 224 ^oC (d); ^1H NMR (DMSO): δ (ppm) 2.75 (s, 6H, $2CH_3$), 4.02 (s, 4H, $2CH_2$), 6.88 (m, 4H, 4CH), 7.26 (m, 4H, 4CH), 7.45 (dd, 2H, 2CH, $^3J_{H-H}$ = 6.5 Hz), 7.51 (d, 2H, 2CH,$^3J_{H-H}$ = 7.8 Hz), 7.56 (d, 2H, 2CH, $^3J_{H-H}$ = 1.2 Hz), 7.58 (d, 2H, 2CH, $^3J_{H-H}$ = 1.3 Hz), 7.60 (d, 2H, 2CH, $^3J_{H-H}$ = 1.4 Hz), 7.64 (m, 2H, 2CH), 7.69 (m, 2H, 2CH), 7.78 (d, 2H, 2CH, $^3J_{H-H}$ = 1.7 Hz), 8.27 (d, 2H, 2CH, $^3J_{H-H}$ = 8.4 Hz), 8.48 (d, 2H, 2CH,$^3J_{H-H}$ = 4.8 Hz), 8.64 (t, 4H, $2NH_2$,$^3J_{H-H}$ = 4.8), 13.42 (s, 1H, 2NH). IR: ν/cm^{-1}; 3156, 2975, 1602, 1569, 1506, 1431, 1390,

1325, 1237, 1163, 1066, 1035, 931, 874, 764, 675, 644, 601, 572, 546, 524, 462, 409. UV-Vis: λ_{max} (MeOH)/nm; 209, 256, 287, 360.

2.4 Anti-bacterial activity

In-vitro, anti-bacterial activities of the synthesized zinc complexes and their parent ligands were evaluated by examining the inhibition of the bacterial growth by agar diffusion method against five Gram-positive (*Staphylococcus aureus, Micrococcus luteus, Bacillus subtilis, Enterococcus faecalis and Staphylococcus epidermidis*) and four Gram-negative bacteria (*Pseudomonas aeruginosa, Klebsiella pneumonia, Escherichia coli, Proteus mirabilis*).

The sterile saline solution (0.9 % of NaCl) was prepared and used to dissolve single bacterial colonies until the suspended cells reached the turbidity of McFarland 0.5 Standard. On the surface of Mueller Hinton nutrient agar, the bacterial inoculum was spread by using a sterile cotton swab. In the agar plate, 6 mm in diameter wells were made by using sterile glassy borer, Figure 14 [48, 75].

Zinc complexes were dissolved in in DMSO (6 mg/ml), and 25 μL of each one was added into respective wells in the plates, immediately the plates were incubated at 37 °C for 24 h.

Gentamicin (G) and Erythromycin (E) were used as positive control and DMSO was used as negative control. The anti-bacterial activity of the complexes was determined by measuring the (inhibition zone diameter) in millimeter.

The results were determined by calculating the average of three trials and were stated as average ± standard deviation[47].

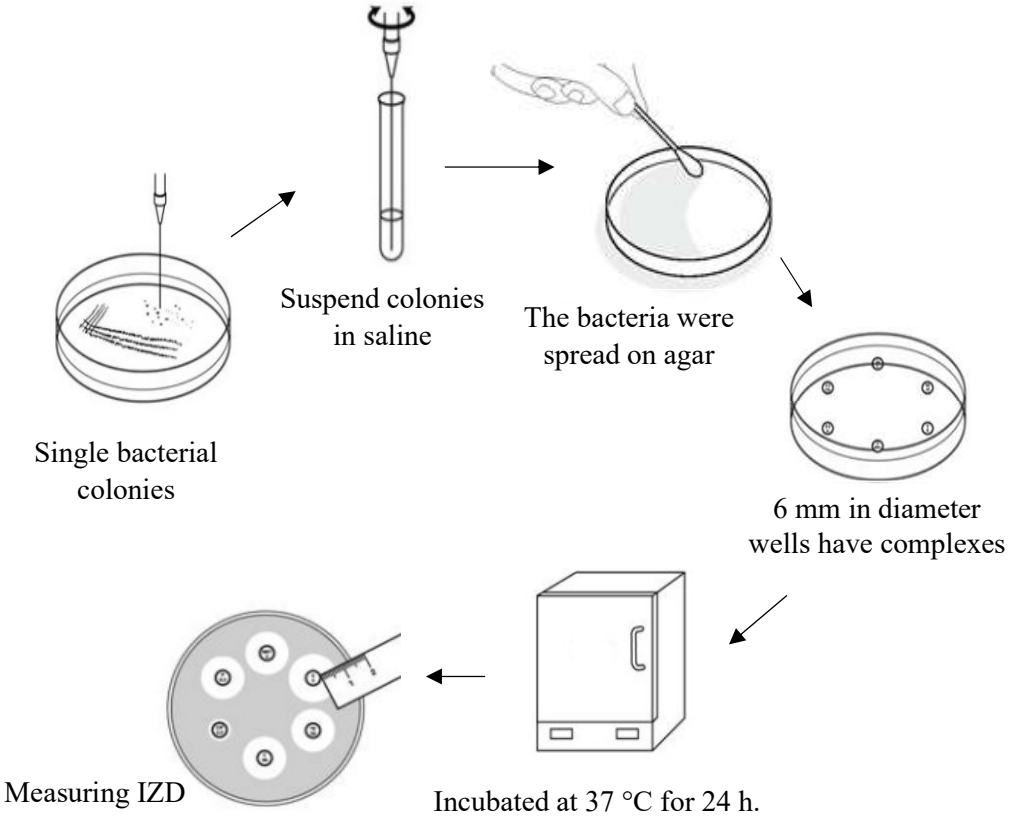

Figure 14: Agar diffusion experiment.

2.5 BNPP hydrolysis

To test the catalytic activity of the Zn complexes, kinetic measurements of BNPP hydrolysis were performed in optimum conditions in twice or three repeated experiments. Agilent 8453 UV-Vis spectrophotometer was used to measure the absorbance of released p-nitrophenol from BNPP hydrolysis vs. time at 400 nm (ε = 13400 L/mol cm)[79,80,81].

HEPES buffer, (4-(2-hydroxyethyl)-1-piperazineethanesulfonic acid), was prepared at different pH with 50 μM concentration by dissolving it in a minimum amount of DW and the final pH of each solution was adjusted with HCl or NaOH to the required pH. Subsequently, BNPP was dissolved in the buffer to obtain 1.0 x 10^{-4} M solution and the volume was adjusted to 100 ml in a 100 ml volumetric flask[79, 81].

Zn complexes were prepared in MeOH or DMSO solution with different concentrations (1.0 x 10^{-4}, 2.0 x 10^{-4} M). After that, 1.5 ml of the Zn complex was immediately combined with 1.5 ml of BNPP solution in a quartz cell at constant temperature (25, 37, 40 °C) for each experiment and the kinetic data was collected[75].

The effect of BNPP concentration on the hydrolysis was measured by preparing different concentrations 1 x 10^{-4}, 2 x 10^{-4}, 1 x 10^{-3} M solutions under the optimum conditions and the concentration of the enzymes (complexes) remain constant. Moreover, the slope of the plot of p-nitrophenol concentration against time is the initial rate (V_0); [$(rate)_0 = (dc/dt)_0 = (dA/dt)_0/\varepsilon$][82,83].

3. Results and discussion

3.1 Synthesis of zinc piroxicam complexes

The zinc piroxicam complexes were obtained by reflux through reaction of 2 equivalents of NaOH and 2 equivalents of piroxicam to form mono anionic piroxicam (Pir^-) solution then 1 equivalent of $Zn(CH_3COO)_2 \cdot 2H_2O$ was reacted with that solution.

The resulting solution was reacted with different molar ratios of nitrogen-based ligands to form zinc piroxicam complexes (**1-4**) as shown in Scheme 2. Table 4 shows the physical properties and the percentage yields of the complexes (**1-4**).

Scheme 2: Synthesis of complexes **1-4**.

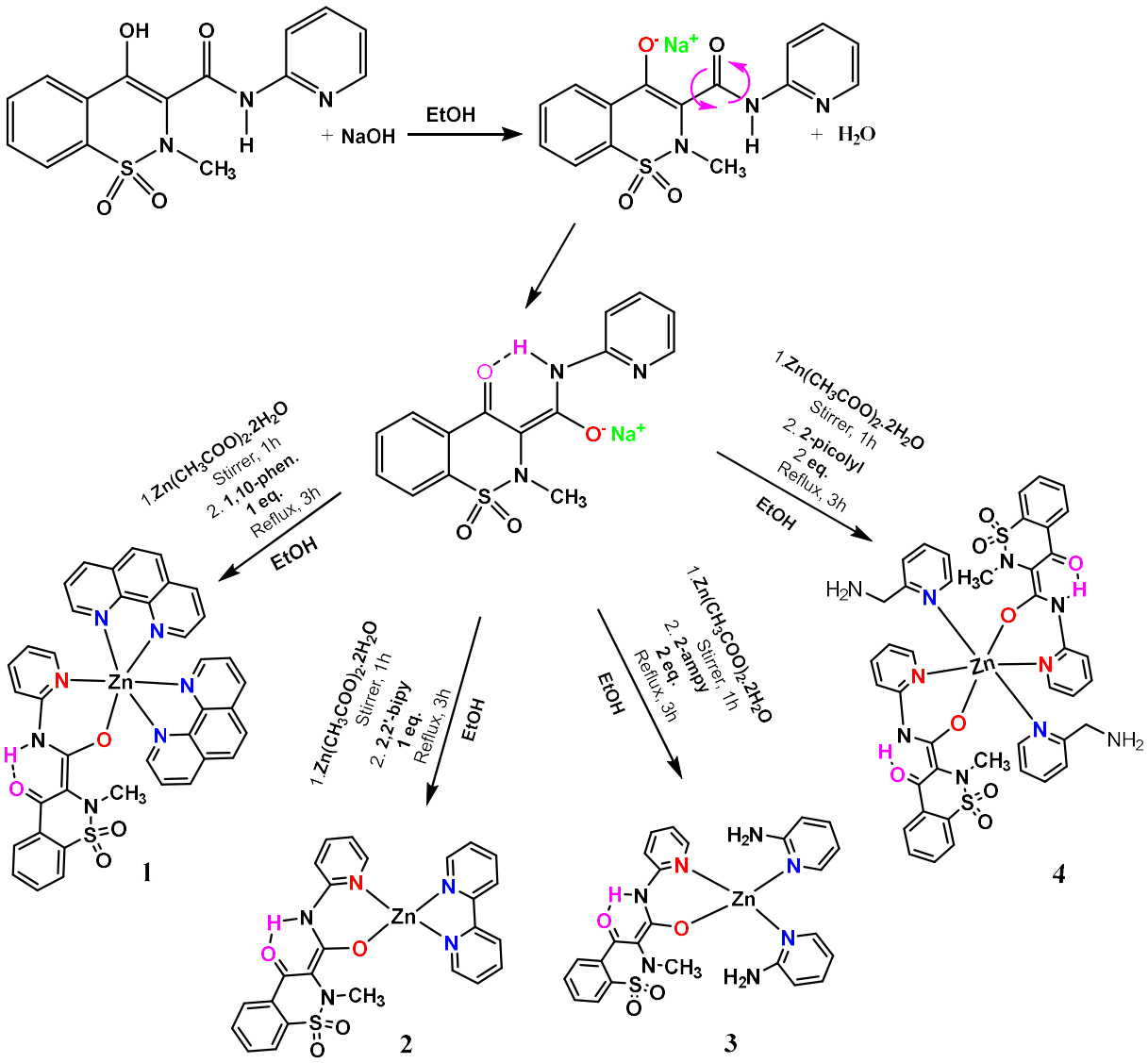

Table 4: Physical properties and % yields of complexes **1-4**.

Complex	Color	m.p (°C)	% Yield	Solubility
[Zn(Pir)(1,10-phen)$_2$] **(1)**	Yellow	172[d]	74	MeOH, chloroform, slightly (Acetone, dichloromethane, MeOH), DMSO, DMF.
[Zn(Pir)(2,2'-bipy)] **(2)**	Yellow	82-85	64	EtOH, MeOH, ACN, chloroform, Acetone, dichloromethane, DMSO, DMF.
[Zn(Pir)(2-ampy)$_2$] **(3)**	Light-yellow	51-53	71	DMSO, DMF.
[Zn(Pir)$_2$(2-picolyl)$_2$] **(4)**	Yellow	224[d]	88	MeOH, EtOH, Acetone, dichloromethane, DMSO, DMF.

[d] : decomposed

3.2 Infrared spectroscopy

Tables 5 showed the peaks assignment and their frequencies of the prepared zinc complexes, where the IR spectra in the range of (400-4000) cm^{-1} were used to characterize the prepared zinc complexes.

In the IR spectrum of piroxicam, prominent peaks appearing at 1628 and 1574 cm^{-1} were due to $\nu(C{=}O)_{amide}$ and $\nu(C{=}N)_{pyr,}$ respectively. Comparison of the IR spectrum of the zinc complex shown in Figure 15, these peaks shift to 1622 and 1572 cm^{-1}, which indicates that piroxicam is coordinated to the metal atom through the pyridyl nitrogen and the amide oxygen atoms. The N–H stretching vibration which is a sharp peak in piroxicam changes to a broad peak in the spectrum of the Zn complex due to a strong intermolecular hydrogen bonding between the $(N–H)_{amide}$ and $(O^{-})_{enolate}$ of the piroxicam in the Zn(II) complex[84]. Other complexes show almost similar results. Finally, peaks of metal coordination to oxygen and nitrogen *ν*(M-O) and *ν*(M-N) appeared at common range (430-474) cm^{-1} and (524-576) cm^{-1}, respectively[85,64].

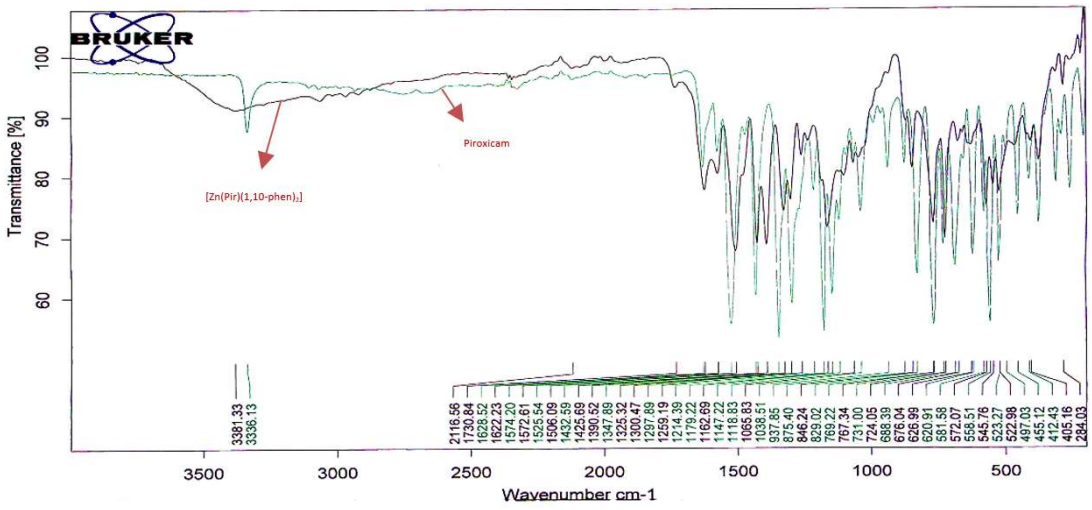

Figure 15: IR spectrum of piroxicam and complex **1**.

Table 5: Assignment frequencies (in cm^{-1}) of piroxicam and complexes **1-4**.

Assignments	Pir	Complex **1**	Complex **2**	Complex **3**	Complex **4**
ν(N–H)	3336	-	-	-	-
$\nu(C{=}O)_{amide}$	1628	1622	1621	1620	1602
ν (C=C)	1526	1506	1505	1507	1506
$\nu(C{=}N)_{pyr}$	1574	1572	1572	1568	1569
O----H——N Strong intermolecular hydrogen bonding	-	3381	3384	3378	3156
$\nu_s(NH_2)$	-	-	-	3378	-
$\nu_{as}(NH_2)$	-	-	-	3483	-
ν(Zn-O)	-	405	408	412	408
ν(Zn-N)	-	572	572	571	456

3.3 Electronic absorption spectroscopy

There are three main types of electronic transitions that may be distinguished in coordination chemistry which are classified according to the orbitals involved in transition: d-d transition, intra ligand transitions, and charge-transfer transitions where the charge transfer processes occur

if the migration of electron is from ligand to metal, then the charge transfer is called ligand to metal charge transfer (LMCT) and in the opposite direction, if the electron transfer is from metal to ligand, it is called metal to ligand charge transfer (MLCT)[86,87].

The electronic transition data of complexes **1-4** and their parent ligands are listed in Table 6. The obtained bands at (201-360) nm of all complexes assigned to MLCT transitions not LMCT as well intra ligand transitions. There are no d-d transition bands due to d^{10} configuration of Zn(II) ion which is filled *d* orbitals.

In addition, the results exhibit a similarity between the complexes and their parent ligands bands except small shifts whether blue or red and new resonances are appeared in some complexes.

Figure 16 shows the UV-visible spectrum of complex **1** and its parent ligand. Figures S4-S6 show the UV-visible spectrum of complexes **2**-**4**, (**Appendix B**).

Table 6: UV-visible spectral data for the complexes and their parent ligands (**1-4**).

Complex	λ_{max} (nm)	Parent ligand	λ_{max} (nm)
[Zn(Pir)(1,10-phen)$_2$] **(1)**	201, 226, 265, 360	1,10-phen	201, 229, 264
[Zn(Pir)(2,2'-bipy)] **(2)**	202, 235, 283, 375	2,2'-bipy	203, 295, 375
[Zn(Pir)(2-ampy)$_2$] **(3)**	202, 295, 358	2-ampy	200, 234, 296
[Zn(Pir)$_2$(2-picolyl)$_2$] **(4)**	209, 256, 287, 360	2-picolyl	205, 261

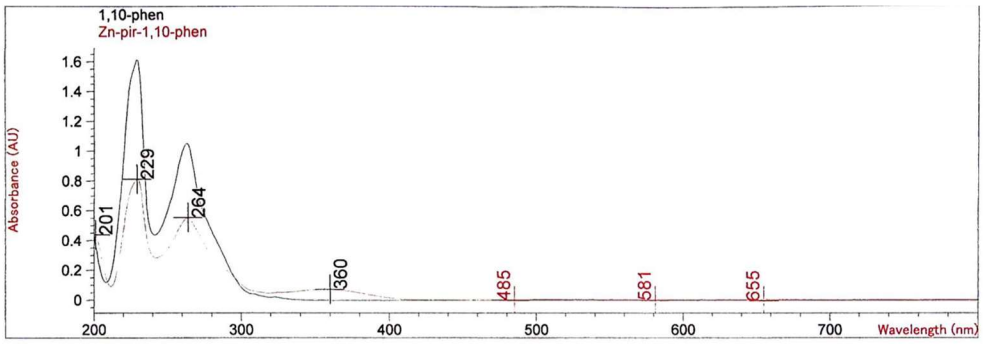

Figure 16: UV-visible spectrum of complex **1** and its parent ligand.

3.4 ^{1}H-NMR

The Nuclear Magnetic Resonance spectroscopy is one of the techniques which is used to determine the structure of the zinc complexes by determining the coordination mode and number of coordination sites of Pir^{-} to the Zn(II) cation. The ^{1}H-NMR spectral data of all complexes are summarized in Tables **S1-S4** (**Appendix C**), the ^{1}H-NMR spectrum of complex **4** is shown in Figure 17, and Figures **S8-S10** shows the ^{1}H-NMR spectra of complexes **1-3**.

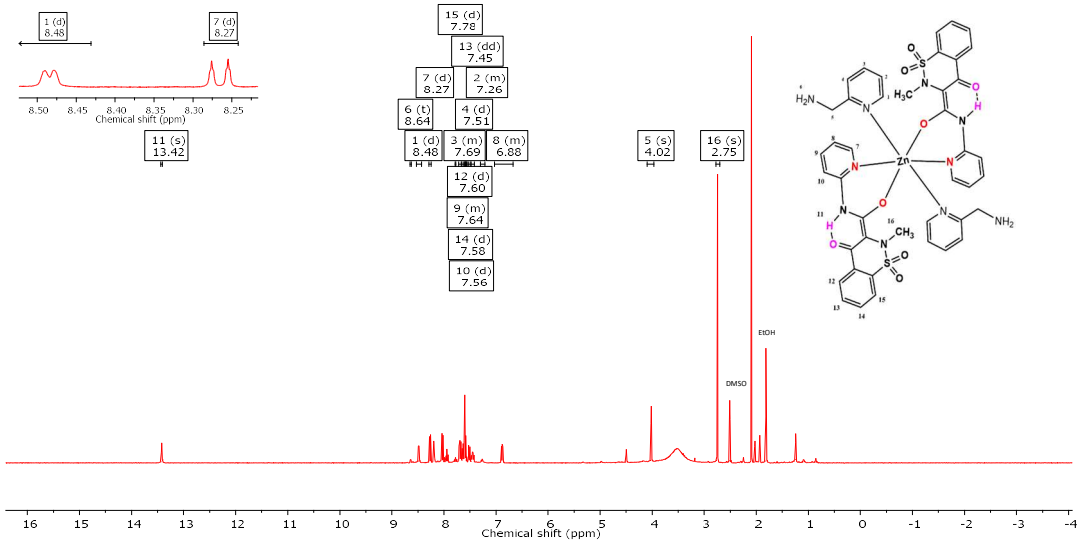

Figure 17: ^{1}H-NMR spectrum of complex **4** in DMSO solution.

Figure S7 shows singlet signals at 10.75 and 16.77 ppm according to NH and OH protons, respectively[88]. As for Zn(II) complexes spectra where are the enol group become deprotonated and there is a twisting around the amide group; via enolate and H of N-H an intermolecular hydrogen bond can be occur and according to that the singlet signal at 16.77 ppm of the proton in OH is disappeared and the peak of N-H shifts toward higher chemical shift, so it absorbs downfield as a broad signal at 13.43, 13.49, 13.39, and 13.42 ppm in complexes **1**, **2**, **3**, and **4**, respectively. The chemical shift of most hydrogens of the pyridyl group in the complexes showed slight upfield shift compared to Pir and the parent ligands due to the Zn(II) coordination effect. In addition, the chemical shift of the sharp singlet peak of CH_3 protons at 2.78 ppm in piroxicam has a small upfield shift in the complexes due to the coordination of Pir^- to Zn(II) cation.

Consequently, the desheilding shift of the N-H peak in the complexes and in the presence of Zn(II) indicates a stronger intermolecular hydrogen bonding. The small changes in the chemical shifts of the hydrogens of the pyridyl group and CH_3 protons indicating that the coordination with Zn(II)

ion is through the N atom of the pyridyl ring (N_{pyr}), and the amide carbonyl (O_{amide}) atom.

The proposed structure of complexes depends on the ratio of ^{1}H-NMR signals' intensities of piroxicam to the nitrogen-based ligands[85].

3.5 Antibacterial activity

The antibacterial activity results reveal that the synthesized zinc complexes (**1-4**) showed good activity against some tested bacterial strains, Figure 17, Figure 18, Table S2, and Table S3 **(Appendix D**).

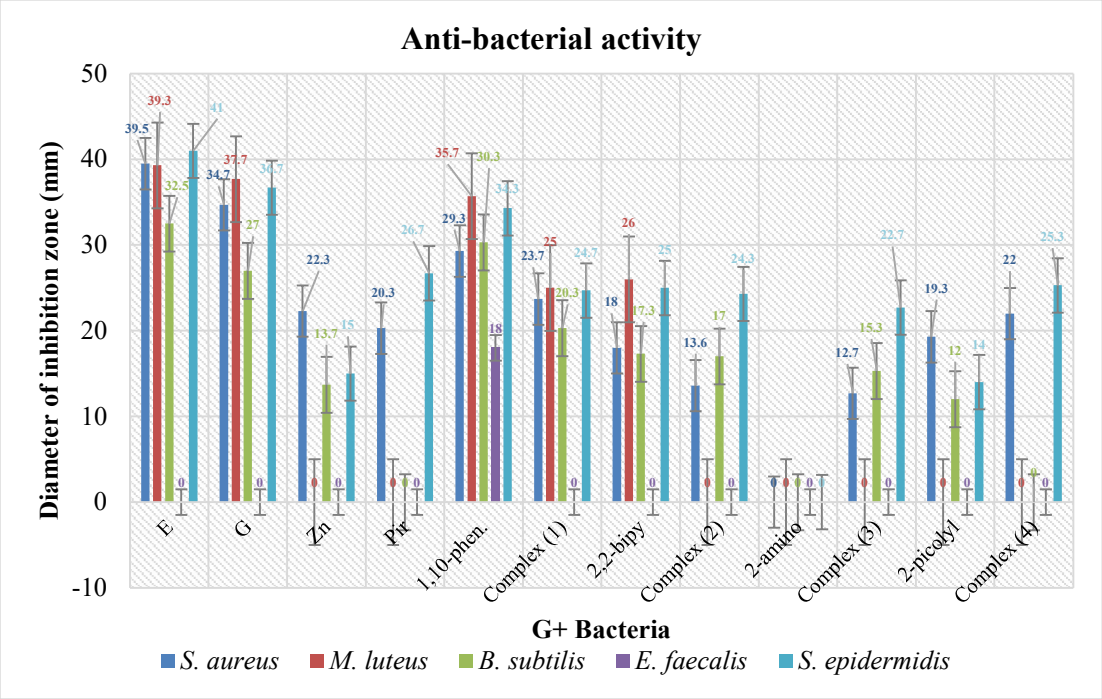

Figure 18: Inhibition zone diameter of complexes **1-4** and their parent ligands against G^{+} bacteria; 6 mg/ml of all species.

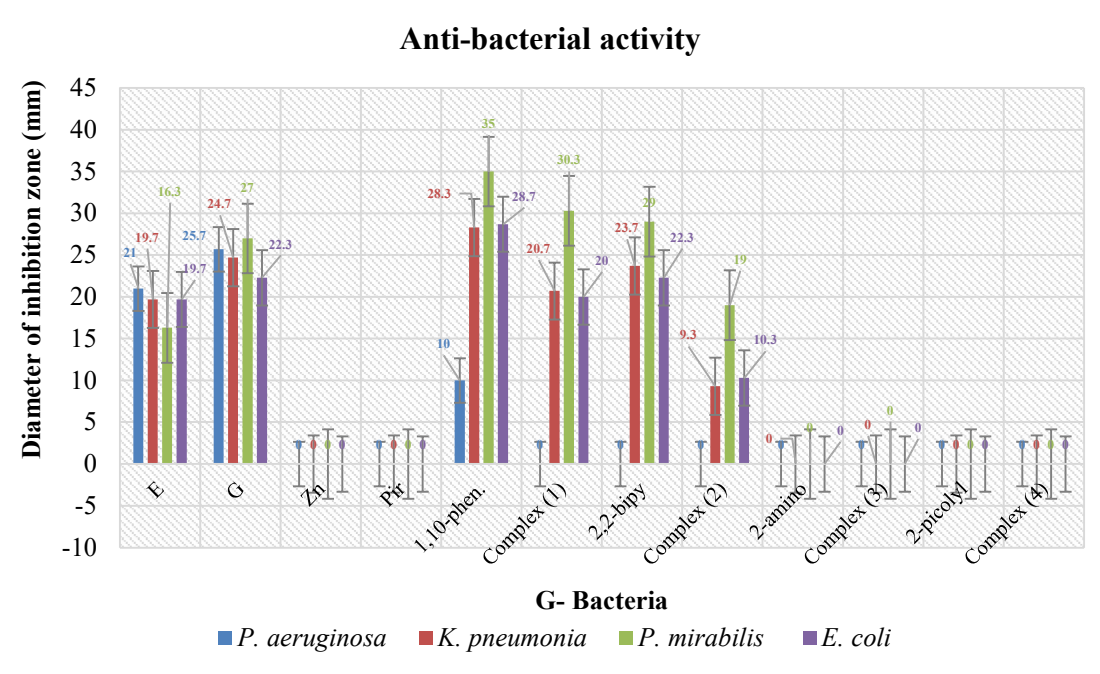

Figure 19: Inhibition zone diameter of complexes **1-4** and other compounds against G^- bacteria; 6 mg/ml of all species.

As a result, DMSO which is used as a negative control and 2-ampy did not show any activity toward all types of the used bacterial species.

Piroxicam showed antibacterial activity against *S. aureus* and *S. epidermidis* with IZD equals 20.3 mm and 26.7 mm, respectively. As well $Zn(CH_3CO_2)_2$ showed anti-bacterial activity against (*S. aureus*, *B. subtilis*, *S. epidermidis*) of Gram-positive bacteria. However, they did not show any activity against all Gram-negative bacteria.

When compared to all complexes, complex **1** showed a higher anti-bacterial activity against all types of bacteria except for *E. faecalis* and *P. aeruginosa* there are no activity but complex **4** showed higher activity against *S. epidermidis*. The IZD range of complex **1** were found between 20.3-30.3 mm. The IZD values of anti-bacterial activity of complex **1** against Gram-positive bacteria were lower than G and E which are the positive controls, while the IZD values against *K. pneumonia* and *E. coli* were higher than E but lower than G and against *P. mirabilis*; the IZD value was higher than G and E. In addition, the parent ligand 1,10-phen showed higher anti-bacterial activity against all type of bacteria compared to complex **1.**

The small molar ratio of 1,10-phen in complex **1** indicate that the overall anti-bacterial activity of this complex come from the complexation process not from the parent ligand only.

Although there is no activity of complex **3** against all Gram-negative bacteria, it showed anti-bacterial activity against *S. aureus*, *B. subtilis*, and *S. epidermidis* of Gram-positive bacteria with IZD equals 12.7, 15.3, and

22.7 mm, respectively which are very lower than G and E, whereas its parent ligand did not show any anti-bacterial activity as mentioned earlier.

Complex **2** showed anti-bacterial activity against some types of Gram-positive bacteria (*S. aureus*, *B. subtilis*, *S. epidermidis*) with IZD vales equal 13.6 mm, 17.0 mm, and 24.3 mm, respectively. These values are very lower than G and E. In addition, it showed anti-bacterial activity against all types of Gram-negative bacteria except *P. aeruginosa* and these values of IZD which are between 9.3-19.0 mm were lower than G and E values but 19.0 mm which is the IZD value of *P. mirabilis* higher than E.

The parent ligand 2,2'-bipy showed higher anti-bacterial activity against all tested bacterial strains in compared to its complex.

Complex **4** and its parent ligand did not show any activity against any type of Gram-negative bacteria. However, against Gram-positive bacteria, complex **4** showed activities against *S. aureus* and *S. epidermidis* with IZD values equal 22.0 and 25.3 mm, respectively, where these values are lower than G and E values. 2-picolyl showed anti-bacterial activity compared to its complex against *B. subtilis* with IZD value equals 12.0 mm, and lower

against *S. aureus* and *S. epidermidis* with IZD values equal 19.3 and 14.0 mm, respectively.

The highest IZD value was for complex **1** against *P. mirabilis* in compared to all complexes. In addition, only complex **1** showed inhibition activity against *M. luteus* with IZD value equals 25.0 mm compared to all zinc complexes.

As shown in the Tables and Figures of antibacterial activity, most of prepared complexes showed anti-bacterial activity against Gram-positive bacteria compared to Gram-negative bacteria which may be due to the distinctive structure of Gram-negative bacteria.

Figure 20 shows the differences in the protective outer membrane (OM) between Gram negative bacteria and Gram-positive bacteria; Gram-positive bacteria lack this part. OM contains lipopolysaccharide and it is a lipid bilayer. It acts as a permeability barrier and this feature prevents the arrival of noxious compounds to the cell wall[89,90 ,91].

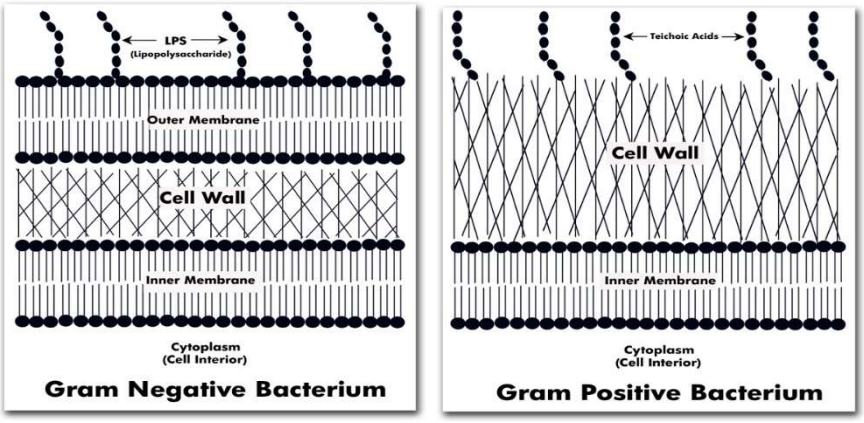

Figure 20: Cross-sections of the cell wall and cell membrane of Gram-positive bacteria and Gram-negative bacteria[92].

The complexation of zinc piroxicam and nitrogen-based ligands showed different IZD values when compared with Zn, piroxicam and the parent ligands. As shown, some complexes showed IZD values lower or higher than another compounds, and sometimes there is no inhibition when compared to G and E, Figure 21.

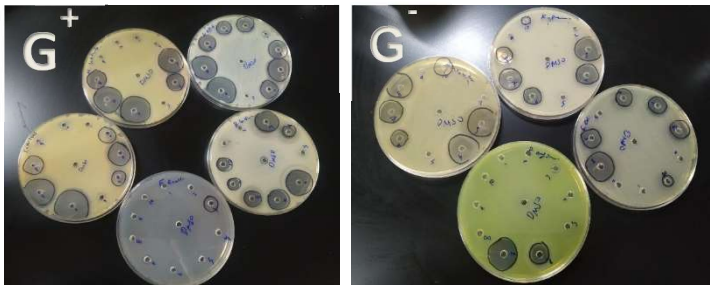

Figure 21: *In vitro* agar diffusion method.

The various results of antibacterial activity were affected by the metal, and the different nitrogen-based ligands. The effect of each one appears to strongly increase the antibacterial activity of these complexes[93,94].

3.6 BNPP catalytic hydrolysis

Zn complexes were used for BNPP hydrolysis. The rate of hydrolysis was studied under optimum conditions (different temperatures, pH, and concentrations). The optimum conditions were obtained by changing one of the above factors and keeping the other two constants.

3.6.1 Effect of concentration on BNPP hydrolysis

Figures 22 and 23 show BNPP hydrolysis at different concentrations of complex **1** and **3**, respectively at constant pH, temperature and BNPP concentration. The initial rates (V_o) for complex **1** equal 9×10^{-10} and 3×10^{-9} mol/L.s for 1×10^{-4} and 2×10^{-4} M concentrations, respectively. In addition, the initial rates of complex **3** equal 4×10^{-9} and 5×10^{-9} mol/L.s for 1×10^{-4} and 2×10^{-4} M concentrations, respectively. V_o values were determined by measuring the absorbance of p-nitrophenol vs. time at 400 nm.

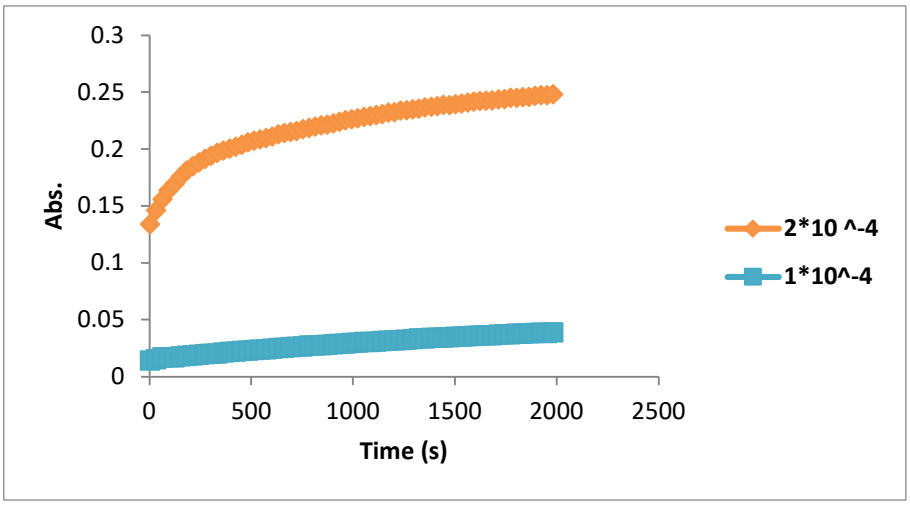

Figure 22: BNPP hydrolysis at different concentrations of complex **1** in MeOH/HEPES buffer solution under certain conditions ([BNPP] = 1 x 10^{-4} M, pH = 7.52 and T = 40 ˚C).

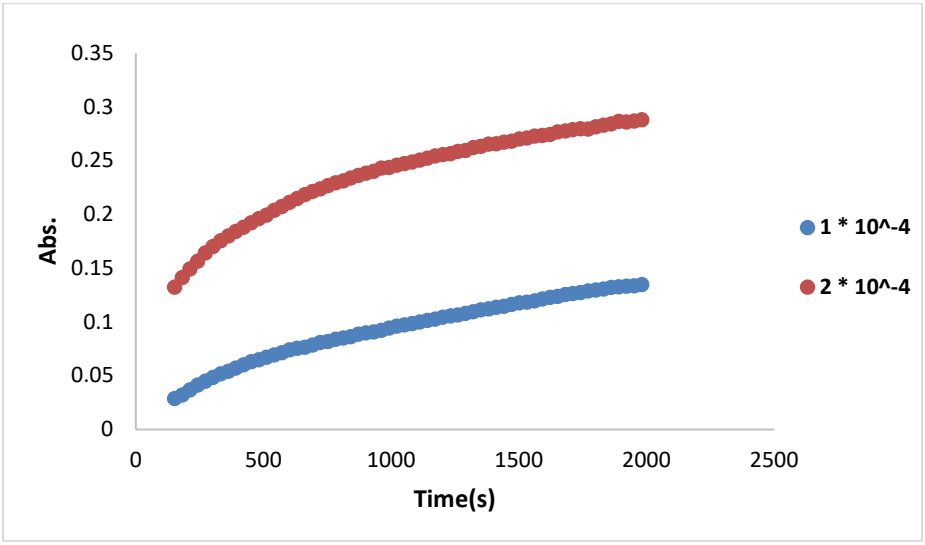

Figure 23: BNPP hydrolysis at different concentrations of complex **3** in DMSO/HEPES buffer solution under certain conditions ([BNPP] = 1 x 10^{-4} M, pH = 7.53 and T = 37 ˚C).

3.6.2 Effect of pH on BNPP hydrolysis

The relationship of absorbance vs. time in Figure 24 show the BNPP hydrolysis at different pH values of complex **1** where the temperature, concentrations of BNPP and complex **1** are constant. At pH 7.52 the initial rate equal 7 x 10^{-9} mol/L.s. Moreover, V_o at pH 7.93 and pH 7.07 equal 2 x 10^{-9} and 5 x 10^{-10} mol/L.s, respectively. The maximum V_o was at pH 7.52 for complex **1**.

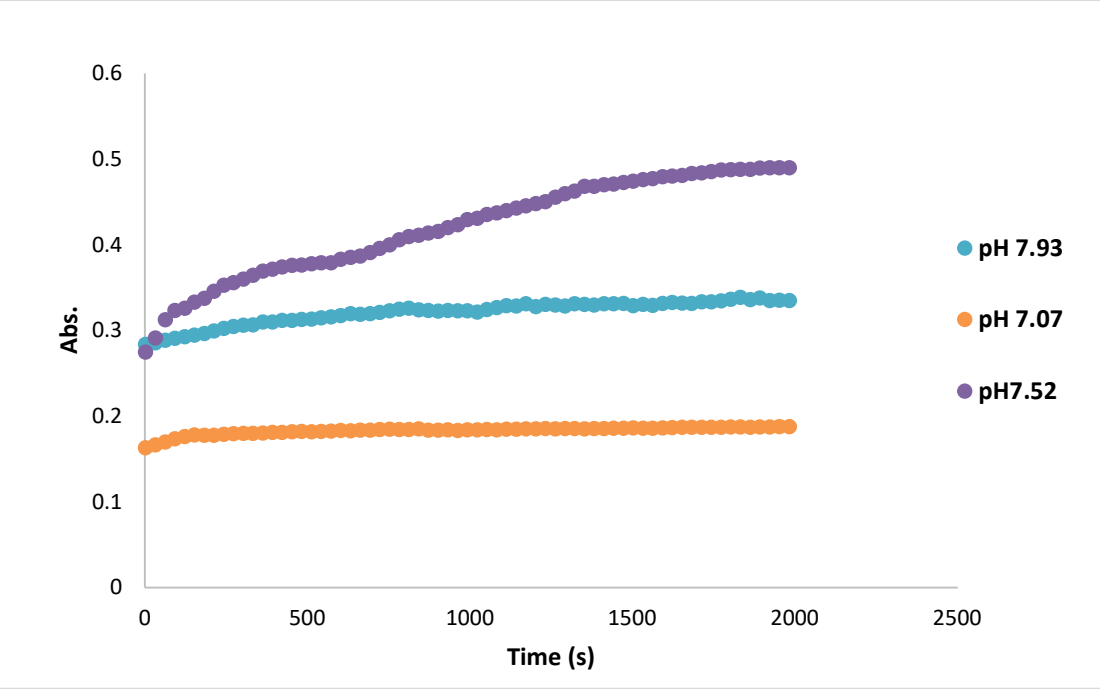

Figure 24: BNPP hydrolysis at different pH values of complex **1** in MeOH/HEPES buffer solution under certain conditions ([BNPP] = 1 x 10^{-4} M, [complex **1**] = 2 x 10^{-4} M, and T = 25 °C).

Figure 25 and Figure 26 show the absorbance vs. time measurements for complexes **3** and **4**, respectively at different pH values and a temperature at 37 °C, and constant concentration of both BNPP and complexes. The V_o values are **4** x 10^{-9}, 5 x 10^{-9}, and 3 x 10^{-9} mol/L.s at pH 7.09, pH 7.53, and pH 7.90, respectively for complex **3**. For complex **4**, V_o equal 2 x 10^{-9}, 5 x 10^{-9}, and 3 x 10^{-9} mol/L.s at pH 7.04, pH 7.52, and pH 7.92, respectively. The optimum one was at pH = 7.53 for complex **3**, and pH = 7.52 for complex **4**.

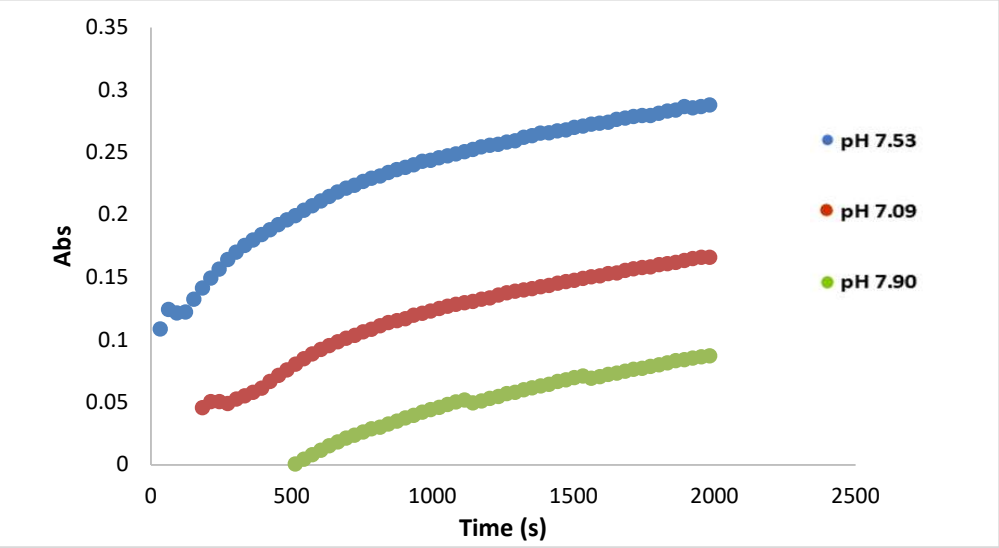

Figure 25: BNPP hydrolysis at different pH values of complex **3** in DMSO/HEPES buffer solution under certain conditions ([BNPP] = 1 x 10^{-4} M, [complex **3**] = 2 x 10^{-4} M, and T = 37 °C).

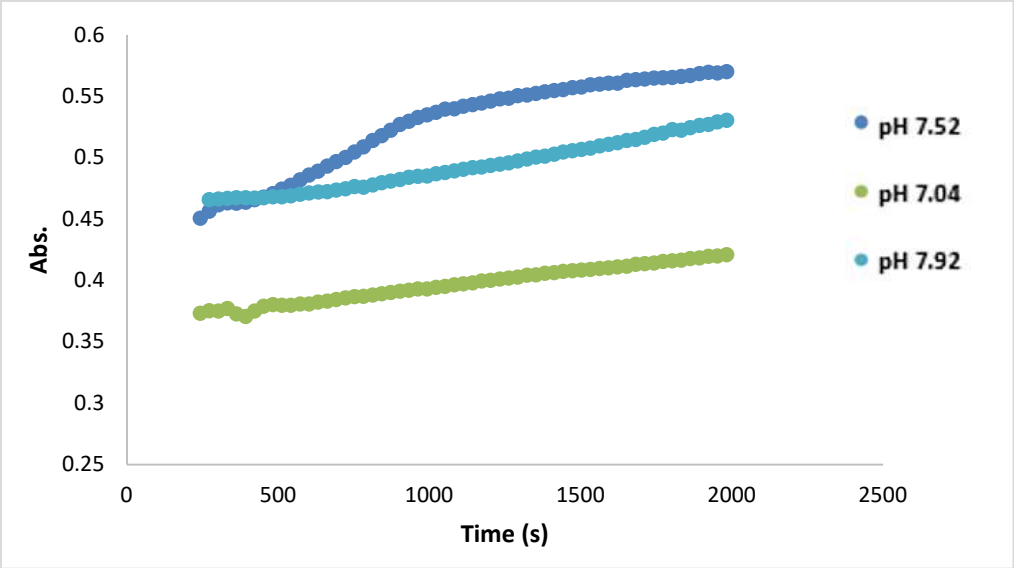

Figure 26: BNPP hydrolysis at different pH values of complex **4** in DMSO/HEPES buffer solution under certain conditions ([BNPP] = 1 x 10^{-4} M, [complex **4**] = 2 x 10^{-4} M, and T = 37 °C).

3.6.3 Effect of temperatures on BNPP hydrolysis

The relationship between absorbance and time at different temperature values for complexes **1**, **3**, and **4** were plotted in Figure 27, 28, and 29, respectively, while the other conditions were constant. The V_o values of complex **1** are 5 x 10^{-10}, 3 x 10^{-9}, and 2 x 10^{-9} mol/L.s at 25, 37, and 40 °C, respectively. And it was equal 1 x 10^{-9}, 4 x 10^{-9}, and 5 x 10^{-9} mol/L.s at T = 25, 37, and 40 °C, respectively for complex **3**. As for complex **4**, the initial rats equal 8 x 10^{-9}, 4 x 10^{-9}, and 3 x 10^{-9} mol/L.s at 25, 37, and 40

°C, respectively. The maximum V_o for these complexes were at 37 °C, 40 °C, and 25 °C for complexes **1**, **3**, and **4**, respectively.

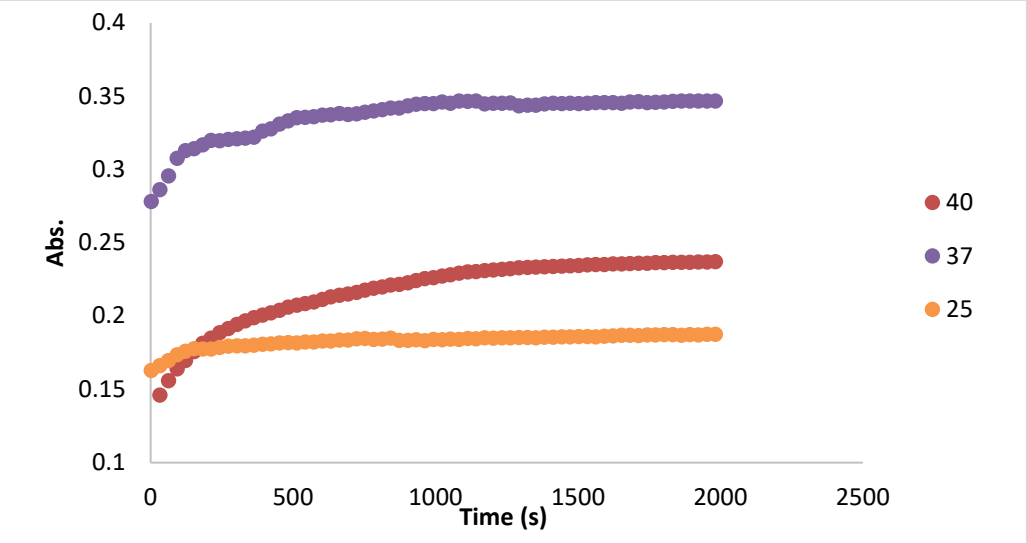

Figure 27: BNPP hydrolysis at different temperature values of complex **1** in MeOH/HEPES buffer solution under certain conditions ([BNPP] = 1 x 10^{-4} M, [complex **1**] = 2 x 10^{-4} M, and pH = 7.52).

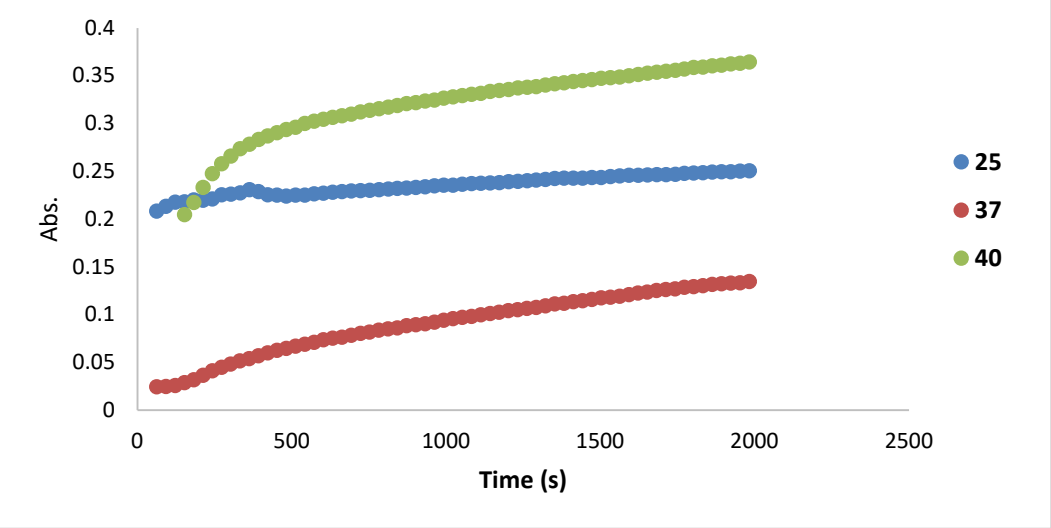

Figure 28: BNPP hydrolysis at different temperature values of complex **3** in DMSO/HEPES buffer solution under certain conditions ([BNPP] = 1 x 10^{-4} M, [complex **3**] = 2 x 10^{-4} M, and pH = 7.53).

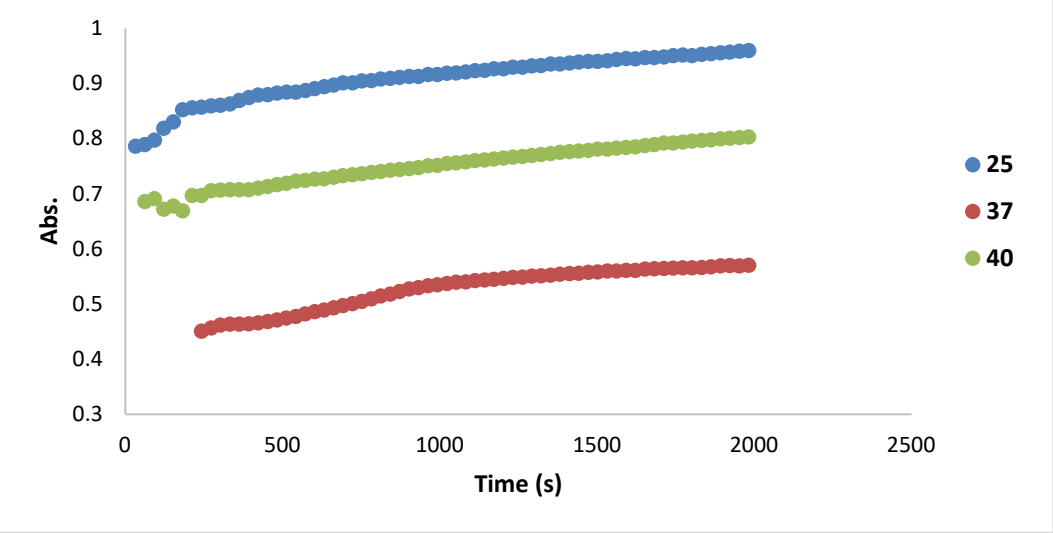

Figure 29: BNPP hydrolysis at different temperature values of complex **4** in DMSO/HEPES buffer solution under certain conditions ([BNPP] = 1 x 10^{-4} M, [complex **4**] = 2 x 10^{-4} M, and pH = 7.52).

According to Michaelis-Menten (MM) equation ($1/V_o = 1/V_{max} + K_m/V_{max}[BNPP]$, which is the used model for enzymatic reactions[81], Figure 30 shows the relationship of the initial rate and the concentration of BNPP of complex **4**. The other complexes (**1**-**3**) showed the same relation and the kinetic parameters of the phosphate diester group hydrolysis for all complexes at different BNPP concentrations are tabulated in Table 7.

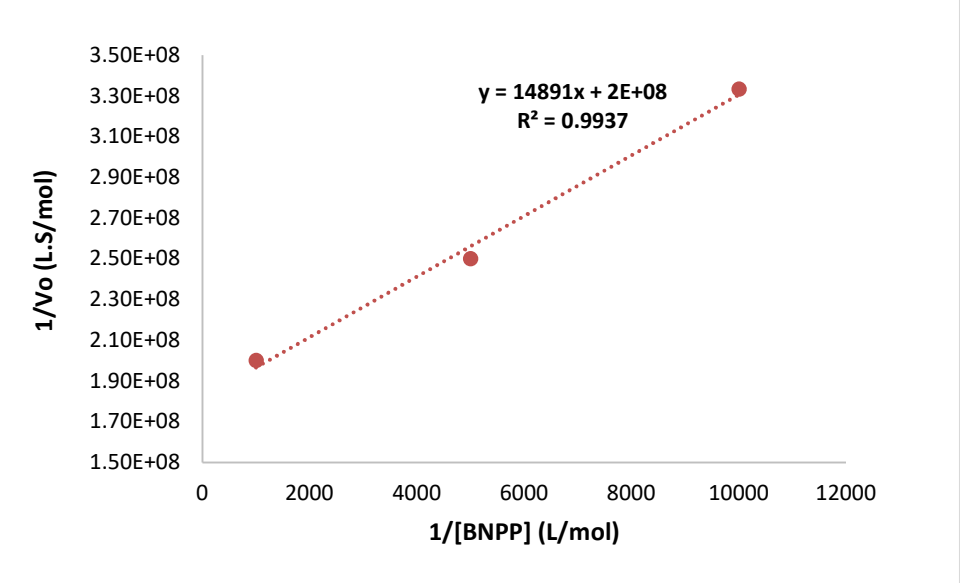

Figure 30: Second order rate for complex **4** with different [BNPP] under the selected conditions (pH = 7.52, T = 25 ºC and [complex **4**] = 2×10^{-4} M).

Table 7: Kinetic parameters of the BNPP hydrolysis for complexes **1-4** at different BNPP concentrations.

Concentration of complexes (M)		Concen-tration of BNPP (M)	V_o (mol/L.s)	V_{max} (mol/L.s)	K_m (mol/L)	K_{cat}^* (s^{-1})	2-order rate $K_{BNPP}^\#$ (L/mol.s)
1	2×10^{-4}	1×10^{-3}	4×10^{-9}	1.4×10^{-8}	1.2×10^{-3}	7×10^{-5}	0.06
1	2×10^{-4}	2×10^{-4}	3×10^{-9}				
1	2×10^{-4}	1×10^{-4}	1×10^{-9}				
2	2×10^{-4}	1×10^{-3}	8×10^{-9}	1×10^{-7}	4.2×10^{-3}	5×10^{-4}	0.12
2	2×10^{-4}	2×10^{-4}	4×10^{-9}				
2	2×10^{-4}	1×10^{-4}	2×10^{-9}				
3	2×10^{-4}	1×10^{-3}	5×10^{-9}	5×10^{-9}	3.1×10^{-5}	2.5×10^{-5}	0.81
3	2×10^{-4}	2×10^{-4}	4×10^{-9}				
3	2×10^{-4}	1×10^{-4}	2×10^{-9}				
4	2×10^{-4}	1×10^{-3}	5×10^{-9}	5×10^{-9}	7.4×10^{-5}	2.5×10^{-5}	0.34
4	2×10^{-4}	2×10^{-4}	4×10^{-9}				
4	2×10^{-4}	1×10^{-4}	3×10^{-9}				

(*) $K_{cat} = V_{max}/[complex]$, (#) $K_{BNPP} = K_{cat}/K_m$

The results of using Zn complexes as catalysts in this study show that the rate of BNPP hydrolysis using complexes **1-4** was in the following order: **3** (40 ºC) > **4** (25 ºC) > **2** (37 ºC) > **1** (37 ºC).

4. Conclusions

Four new zinc complexes with piroxicam and N-based ligands were synthesized and structurally characterized by IR, UV-vis, and ^{1}H-NMR spectroscopy. These complexes were: [Zn(Pir)(1,10-phen)$_2$] (**1**),

[Zn(Pir)(2,2'-bipy)] (**2**), [Zn(Pir)(2-ampy)$_2$] (**3**), and [Zn(Pir)$_2$(2-picolyl)$_2$] (**4**).

The results showed that the piroxicam in all complexes chelates the Zn(II) cation through the N atom of the pyridyl ring and the amide carbonyl as a bidentate chelating ligand.

All of the zinc piroxicam complexes showed anti-bacterial activity against all tested bacteria strains except complexes **3** and **4** did not show any activity against all tested Gram-negative bacteria. Complex **1** showed a higher anti-bacterial activity against all types of the selected bacteria except *E. faecalis* and *P. aeruginosa* there are no activity whereas the highest IZD value was for complex **1** against *P. mirabilis* compared to all complexes. In addition, only complex **1** showed inhibition activity against *M. luteus* with IZD value equals 25.0 mm compared to complexes **2-4**.

The results of using these new complexes as catalysts in the BNPP hydrolysis showed following trend of the rate of hydrolysis: **3** (40 ^{o}C) > **4** (25 ^{o}C) > **2** (37 ^{o}C) > **1** (37 ^{o}C).

5. References

[1] Ackerman, C. M.; Lee, S.; Chang, C. J., *Anal. Chem.* **2017**, *89*, 22–41.

[2] Chen, C.; Chai, Z.; Gao, Y. Nuclear analytical techniques for metallomics and metalloproteomics; Royal Society of Chemistry: Cambridge, 2010.

[3] Trefil, J. (2007). McDougal Littell Science: Focus on Physical Sciences. Evanston, IL: McDougal Littell. p. 340.

[4] Khurshid, S. J.; Qureshi, I. H. The Role of Inorganic Elements in Human Body. Nucleus 1984, *21*, 3–23.

[5] Kaim, W. Bioinorganic chemistry: Inorganic elements in the chemistry of life an introduction and guide; Wiley: Chichester, West Sussex, United Kingdom, 2013.

[6] Al-fartusie, F. S.; Mohssan, S. N., *Indian Journal of Advances in Chemical Science*., **2017**, 127–136.

[7] Skalnaya, M. G.; Skalny, A. V. Essential Trace Elements in Human Health: A Physician'S View. **2018**, 224 p.

[8] Periodic Graphics: Essential Elements for Humans. C&EN Global Enterprise **2019**, *97*, 25–25.

[9] Zingaro, R. How Certain Trace Elements Behave. Environmental Science & Technology, **1979**, *13,* 282–287.

[10] Shyamala I. "Atoms & Life". ASU - Ask A Biologist. 27 September 2009. https://askabiologist.asu.edu/content/atoms-life

[11] Abdull, M.; Chmielnicka, J., *Biological Trace Element Research*, **1990**, *23*.

[12] Pathak, U., M.; Shetty, V.; Kalra, D., *J Adv Oral Res*, **2016**, *7*, 12-20.

[13] Lindh, U. Biological Functions of the Elements. Essentials of Medical Geology 2012, 129–177.

[14] Tang, N.; Skibsted, L. H., *J. Agric. Food Chem.* **2017**, *65* (39), 8727–8743.

[15] Watstein, D. M.; Styczynski, M. P.*ACS Synth. Biol.* **2018**, *7* (1), 267–275.

[16] Subbaiah, L. V.; Prasad, T. N. V. K. V.; Krishna, T. G.; Sudhakar, P.; Reddy, B. R.; Pradeep, T., *J. Agric. Food Chem.* **2016**, *64* (19), 3778–3788.

[17] McCall, K. A.; Huang, Ch.; Fierke, C. A., *The Journal of Nutrition*, **2000**, *130*, 1437S–1446S.

[18] Zalewski, P. D.; Truong-Tran, A. Q.; Grosser, D.; Jayaram, L.; Murgia, C.; Ruffin, R. E., *Pharmacology and Therapeutics*. **2005**, 127–149.

[19] Santos, H. O.; Teixeira, F. J.; Schoenfeld, B. J., *Clinical Nutrition*, **2019**.

[20] Rangan, A. M.; Samman, S., *Nutrients*, **2012**, *4*, 611-624.

[21] Bioactive Food as Dietary Interventions for the Aging Population. 2013.

[22] Arsenault, J. E.; Brown, K. H., *American Journal of Clinical Nutrition*, **2003**, *78*, 1011– 1017.

[23] Solomons, N. W., *Modern Nutrition in Health and Disease*, **1988**, *7*, 238–262.

[24] Dietary Reference Intakes for Vitamin A, Vitamin K, Arsenic, Boron, Chromium, Copper, Iodine, Iron, Manganese, Molybdenum, Nickel, Silicon, Vanadium, and Zinc. 2001.

[25] Hambidge, K. M.; Krebs, N. F., *The Journal of Nutrition*, **2007**, *137*, 1101–1105.

[26] Wani, A. L.; Parveen, N.; Ansari, M. O.; Ahmad, M. F.; Jameel, S.; Shadab, G. G. H. A., *Curr. Med. Res. Pract.* **2017**, *7 (3)*, 90–98.

[27] KIDD, M. T.; FERKET, P. R.; QURESHI, M. A., *World's Poultry Science Journal*, **1996**, *52*, 309-324.

[28] Bagherani, N.; Smoller, B. R., *Glob Dermatol,* **2016***, 3,* 330-336.

[29] Osredkar, J.; Sustar, N., *J of Clinic Toxicol*, **2011**.

[30] Kulg, A., *Annual Review of Biochemistry*, **2010**, *79*, 213-231.

[31] Zinc - Element information, properties and uses: Periodic Table. https://www.rsc.org/periodic-table/element/30/zinc#history (accessed Apr 6, 2020).

[32] Moynier, F. Zinc Isotopes. Encyclopedia of Earth Sciences Series Encyclopedia of Geochemistry 2018, 1524–1527.

[33] Green, A.; Parker, M.; Conte, D.; Sarkar, B., *J. of Trace Elements in Experimental Medicine,* **1998**, *11*, 103-118.

[34] Twedt, D. C., Chelating Agents. Canine and Feline Gastroenterology **2013**, 489–493.

[35] Flora, G.; Mittal, M.; Flora, S. J., Medical Countermeasures—Chelation Therapy. Handbook of Arsenic Toxicology **2015**, 589–626.

[36] Zhou, X.; Pang, X.; Nie, L.; Zhu, C.; Zhuo, K.; Zhuo, Q.; Chen, Z.; Liu, G.; Zhang, H.; Lin, Z.; et al. *Nature Communications*. **2019**.

[37] Casiday, Rachel, and Regina Frey. "Hemoglobin and the heme group: Metal complexes in the blood for oxygen transport." Retrieved March 28 (1998): 2008.

[38] Pinto, I. S. S., Neto, I. F. F., & Soares, H. M. V. M. *Environmental Science and Pollution Research*, **2014**, *21*, 11893–11906.

[39] Darawsheh, M., Abu Ali, H., Abuhijleh, A. L., Rappocciolo, E., Akkawi, M., Jaber, S., Hussein, Y., *European Journal of Medicinal Chemistry*, **2014**, *82*, 152–163.

[40] YADAV, P.; PUROHIT, N., *J. Chem. Sci.,* **2013**, *125*, 165-173.

[41] Patel, M. N.; Parmar, P. A.; Gandhi, D. S.; Thakkar, V. R., *J. of Enzyme Inhibition and Med. Chem*., **2011**, *26*, 359–366.

[42] Shulman, A.; White, D. O., *Chemico-Biological Interactions,***1973**, *6*, 407–413.

[43] Sadeek S.; Refat M., *J Korea Chem,* **2006**, *50*.

[44] Sathiyaraj, S.; Sampath, K.; Butcher, R. J.; Pallepogu, R.; Jayabalakrishnan, C., *European Journal of Medicinal Chemistry*, **2013**, *64*, 81–89.

[45] Singh, H. L.; Varshney, A. K., *Bioinorganic Chemistry and Applications*, **2006**, 1–7

[46] Abu Ali, H., Darawsheh, M. D., & Rappocciolo, E., *Polyhedron*, **2013**, *61*, 235–241.

[47] Abu Ali, H., Shalash, A. M.; Akkawi, M.; Jaber, S., *Applied Organometallic Chemistry*, **2017**, *31*.

[48] Abu Ali, H.; Kamel, S.; Abu Shamma, A., *Applied Organometallic Chemistry*, **2017**, *31*.

[49] Xu, S.; Rouzer, C. A.; Marnett, L. J., *IUBMB Life*, **2014**, *66*, 803–811.

[50] El-Gamel, N. E. A., *Journal of Coordination Chemistry,* **2009***, 62,* 2239–2260.

[51] Meloxicam. (n.d.). Retrieved December 26, 2020, from https://bre.is/dZrU5gL5, Isoxicam. (n.d.). Retrieved December 26, 2020, from https://bre.is/rLYCEEcR, Piroxicam. (n.d.). Retrieved December 26,

2020, from https://bre.is/VoqLKdSa, Tenoxicam. (n.d.). Retrieved December 26, 2020, from https://bre.is/rLYCEEcR.

[52] Moya-Hernández, M. R.; Mederos, A.; Domínguez, S.; Orlandini, A.; Ghilardi, C. A., Cecconi, F.,. Rojas-Hernández, A. *Journal of Inorganic Biochemistry*, **2003**, *95*, 131–140.

[53] Tabrizi, L.; Chiniforoshan, H.; Tavakol, H., *Spectrochimica Acta Part A: Molecular and Biomolecular Spectroscopy,* **2015***, 141,* 16–26.

[54] Campione, E., Paternò, E. J., Candi, E., Falconi, M., Costanza, G., Diluvio, L., … Orlandi, A., *Drug Design, Development and Therapy,* **2015**, *9*, 5843-5850.

[55] Del Bakhshayesh, A. R.; Akbarzadeh, A.; Alihemmati, A.; Nasrabadi, H. T.; Montaseri, A.; Davaran, S.; Abedelahi, A., *Drug Delivery*, **2020**, *27*, 269–282.

[56] Christofis, P.; Katsarou, M.; Papakyriakou, A.; Sanakis, Y.; Katsaros, N.; Psomas, G. *Journal of Inorganic Biochemistry*. **2005**, 2197–2210.

[57] Meek, I. L.; van de Laar, M. A. F. J.; Vonkeman, H. E., *Pharmaceuticals*, **2010**, *3*, 2146-2162.

[58] Abdul-Hussein, Z. R., *Basrah Journal of Science (B),* **2014**, *32*, 166-181**.**

[59] Brogden, R. N.; Heel, R. C.; Speight, T. M.; Avery, G. S., *Drug Evaluations*, **1981**, *22*, 165-187.

[60] Weder, J. E., Dillon, C. T., Hambley, T. W., Kennedy, B. J., Lay, P. A., Biffin, J. R., … Davies, N. M. *Coordination Chemistry Reviews,* **2002***, 232,* 95–126.

[61] Smolková, R., Zeleňák, V., Smolko, L., Kuchár, J., Rabajdová, M., Ferenčáková, M., & Mareková, M. *European Journal of Medicinal Chemistry*, **2018**, *153*, 131–139.

[62] Christofis, P., Katsarou, M., Papakyriakou, A., Sanakis, Y., Katsaros, N., & Psomas, G. *Journal of Inorganic Biochemistry,* **2005***, 99,* 2197–2210.

[63] TITA, B.; RUSU, G.; TITA, D., *REV. CHIM. (Bucharest)*, **2013**, *64*, 472-476.

[64] Jannesari, Z., Hadadzadeh, H., Amirghofran, Z., Simpson, J., Khayamian, T., & Maleki, B. *Molecular and Biomolecular Spectroscopy,* **2015**, *136,* 1119–1133.

[65] Bazzicalupi, C., Bencini, A., Bianchi, A., Fusi, V., Giorgi, C., Paoletti, P., … Zanchi, D*., Inorganic Chemistry*, **1997**, *36*, 2784–2790.

[66] Gómez-Tagle, P., & Yatsimirsky, A. K. *Journal of the Chemical Society*, Dalton Transactions, **2001**, *18*, 2663–2670.

[67] Fry, F. H.; Fischmann, A. J.; Belousoff, M. J.; Spiccia, L.; Brügger, J., *Inorganic Chemistry*, **2005**, *44*, 941–950.

[68] Luong, T. K. N., Mihaylov, T. T., Absillis, G., Shestakova, P., Pierloot, K., & Parac-Vogt, T. N. *Inorganic Chemistry*, **2016**, *55*, 9898–9911.

[69] Suh, J.; Kim, N.; Cho, H. S., *Bioorganic & Medicinal Chemistry Letters,* **1994**, *15*, 1889-1892.

[70] Luong, T. K. N., Shestakova, P., & Parac-Vogt, T. N., *Wells–Dawson polyoxometalate. Dalton Transactions*, **2016**, *45*, 12174–12180.

[71] Bhagavan, N. V.; Ha, C.-E., *Essentials of Medical Biochemistry*, **2015**, 381–400.

[72] Valle-Orta, M., Díaz, D., Dubé, I. Z., Quiñonez, J. L. O., & Guerrero, R. S. (2017). Degradation of bis-p-nitrophenyl phosphate using zero-valent iron nanoparticles. Journal of Physics: Conference Series, 838, 012034.

[73] Jurek, P.; Martell, A., *Inorganica Chimica Acta*, **1999**, *287*, 47–51.

[74] Dhanalakshmi, T., Loganathan, R., Suresh, E., Stoeckli-Evans, H., & Palaniandavar, M., *Inorganica Chimica Acta*, **2011**, *372*, 237–242.

[75] Raymoni, G., & Abu Ali, H., *Applied Organometallic Chemist*ry, **2018**, e4680.

[76] Li, J., Li, H., Zhou, B., Zeng, W., Qin, S., Li, S., Xie, J. *Transition Metal Chemistry*, **2005**, *30*, 278–284.

[77] Mancin, F., Tecilla, P., *New Journal of Chemistry*, **2007**, *31*, 800.

[78] Cai, S., Feng, F., & Liu, F., *Dispersion Science and Technology*, **2015**, *37*, 1170–1177.

[79] Shalash, A.; AbuAli, H. Faculty of Graduate Studies Non-steroidal Zn (II) and Co (II) Sulindac Drugs and Bioactive bacterial Effect , Anti-malarial Effect and The Use as Phosphate Hydrolyzing Enzymes, Birzeit University, **2015**.

[80] Abuhijleh, A., *Polyhedron*, **1997**, *16*, 733–740.

[81] Abu Shamma, A.; Abu Ali, H.; Kamel, S. *Applied Organometallic Chemistry*, **2017**, *32*, 1-12.

[82] Yang, R., Rodriguez-Fernandez, M., St. John, P. C., Doyle, F. J, *Modelling Methodology for Physiology and Medicine*, **2014**, 159–18.

[83] Li, J.; Li, H.; Zhou, B.; Zeng, W.; Qin, S.; Li, S.; Xie, J., *Transit. Met. Chem***. 2005**, *30* , 278–284.

[84] Saadeh, S. M., Arabian Journal of Chemistry , **2013**, *6*, 191–196.

[85] Ammar, J.; Alabdali, F.; Ibrahim, M., *IOSR J. Appl. Chem.* **2014**, *6* , 60–63.

[86] Lever, a. B. P., *J. Chem. Educ.* **1974**, *51*, 612–616.

[87] Endicott, J. F. (2001). Charge-Transfer Excited States of Transition Metal Complexes. Electron transfer in chemistry, 238-270.

[88] By Chemdraw.

[89] Nikaido, H.; Nakae, T. *Advances in Microbial Physiology*, **1980**, *20*, 163-250.

[90] Silhavy, T. J., Kahne, D., Walker, S. *Cold Spring Harbor Perspectives in Biology*, **2010**, *2*, a000414–a000414.

[91] Exner, M., Bhattacharya, S., Christiansen, B., Gebel, J., Goroncy-Bermes, P., Hartemann, P., . . . Trautmann, M. (2017). Antibiotic resistance: What is so special about multidrug-resistant Gram-negative bacteria? GMS Hygiene Infection Control, 12.

[92] Microchem Laboratory. (n.d.). What is the Difference Between Gram Positive and Gram-Negative Bacteria? Retrieved December 26, 2020, from https://bre.is/dewBLrNg.

[93] Nair, R., Shah, A., Baluja, S., & Chanda, S. *Journal of the Serbian Chemical Society,* **2006***, 71,* 733–744.

[94] Claudel, M; Schwarte, J. V.; Fromm, K. M.; *Chem*., **2020**, *2*, 849-899.

6. Appendices

Appendix A: Infrared spectra of complexes

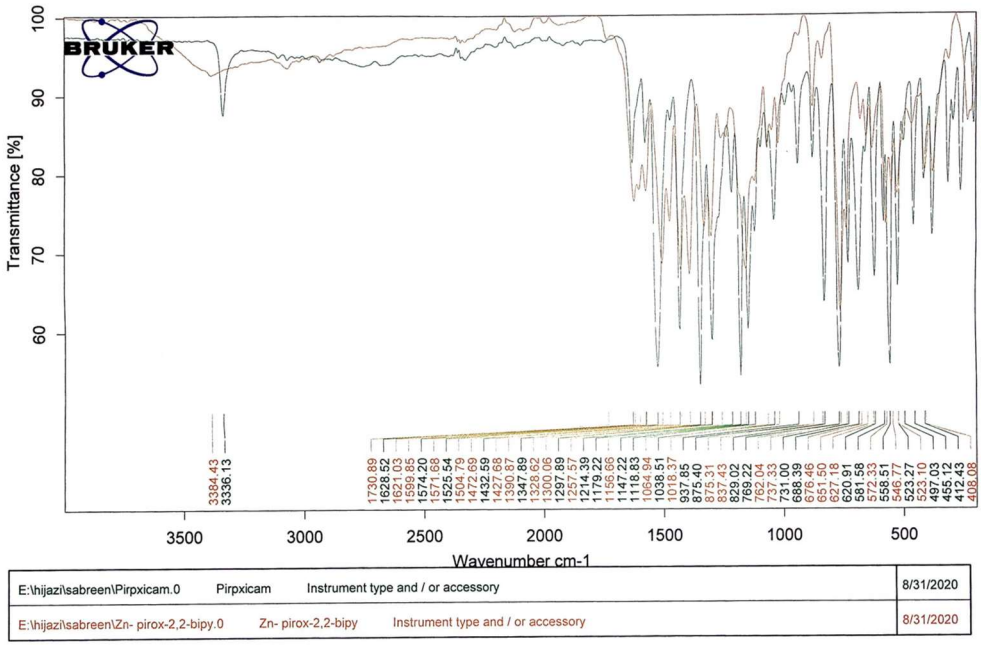

Figure S1: IR spectrum of piroxicam and complex **2.**

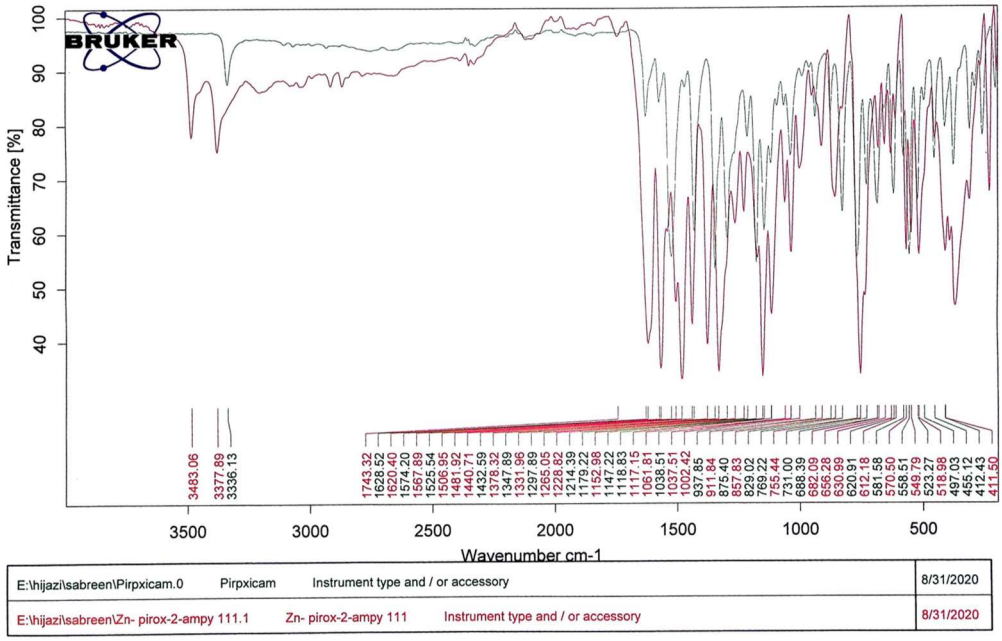

Figure S2: IR spectrum of piroxicam and complex **3.**

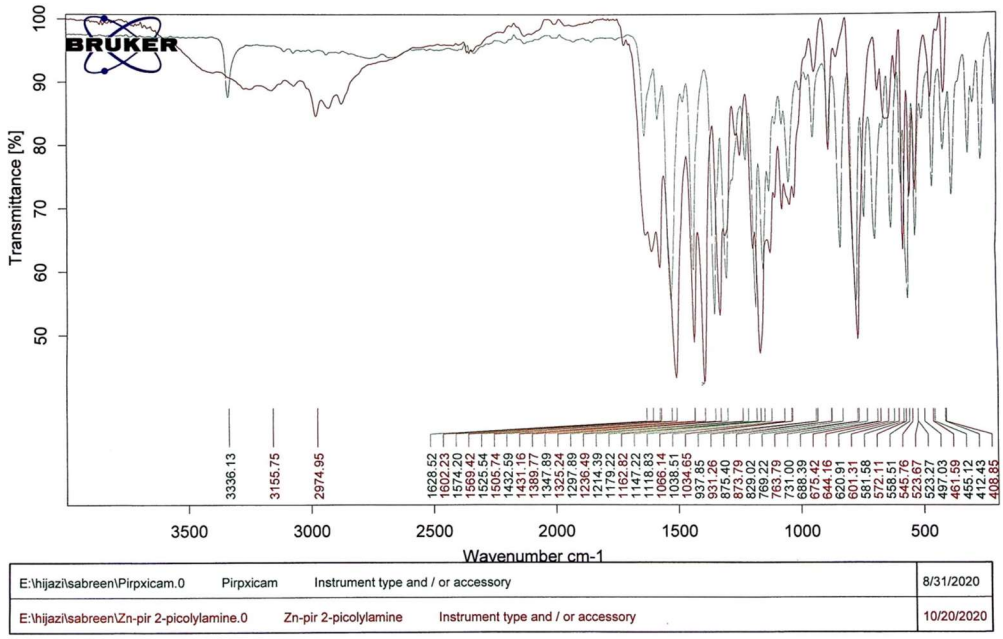

Figure S3: IR spectrum of piroxicam and complex **4.**

Appendix B: Electronic absorption spectroscopy spectra

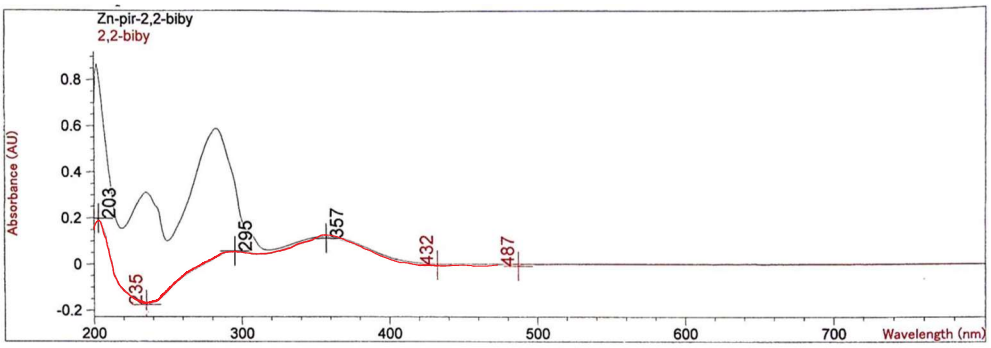

Figure S4: UV-visible spectrum of complex **2** and its parent ligand.

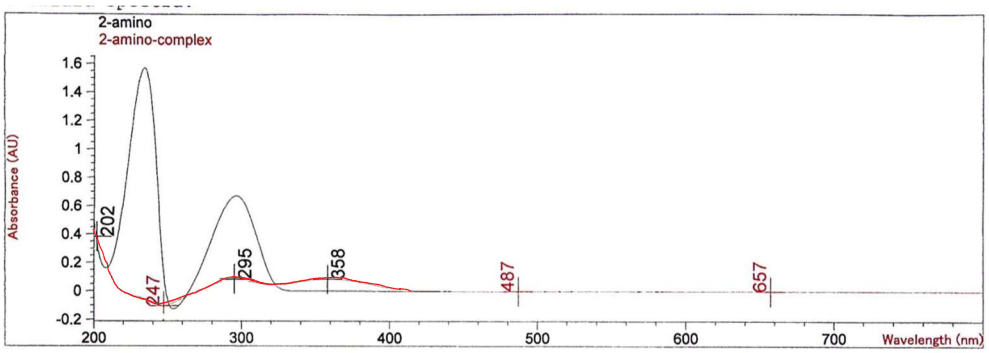

Figure S5: UV-visible spectrum of complex **3** and its parent ligand.

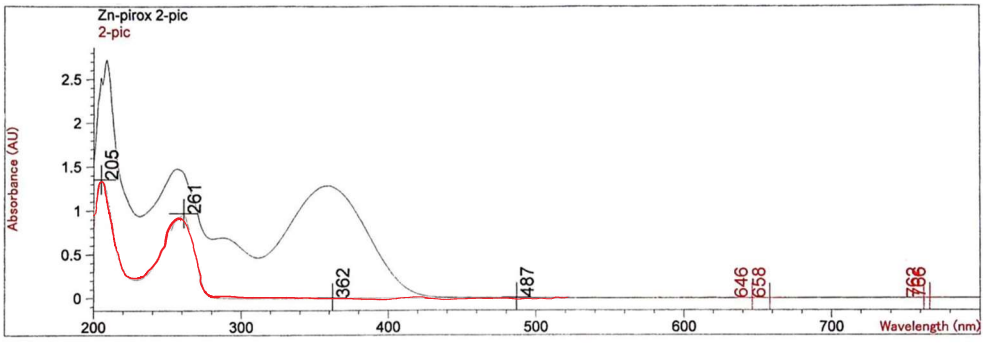

Figure S6: UV-visible spectrum of complex **4** and its parent ligand.

Appendix C: ^{1}H-NMR spectral data

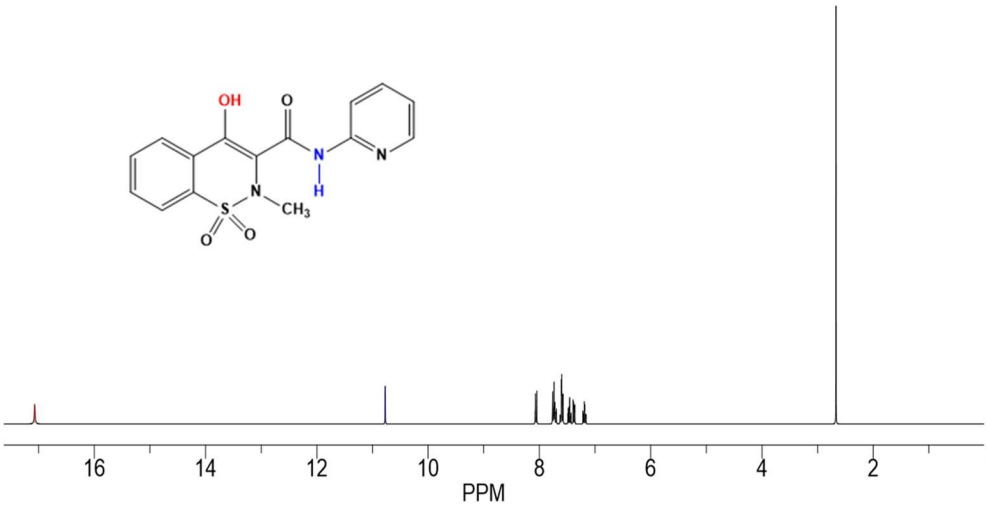

Figure S7: ^{1}H-NMR spectrum of piroxicam.

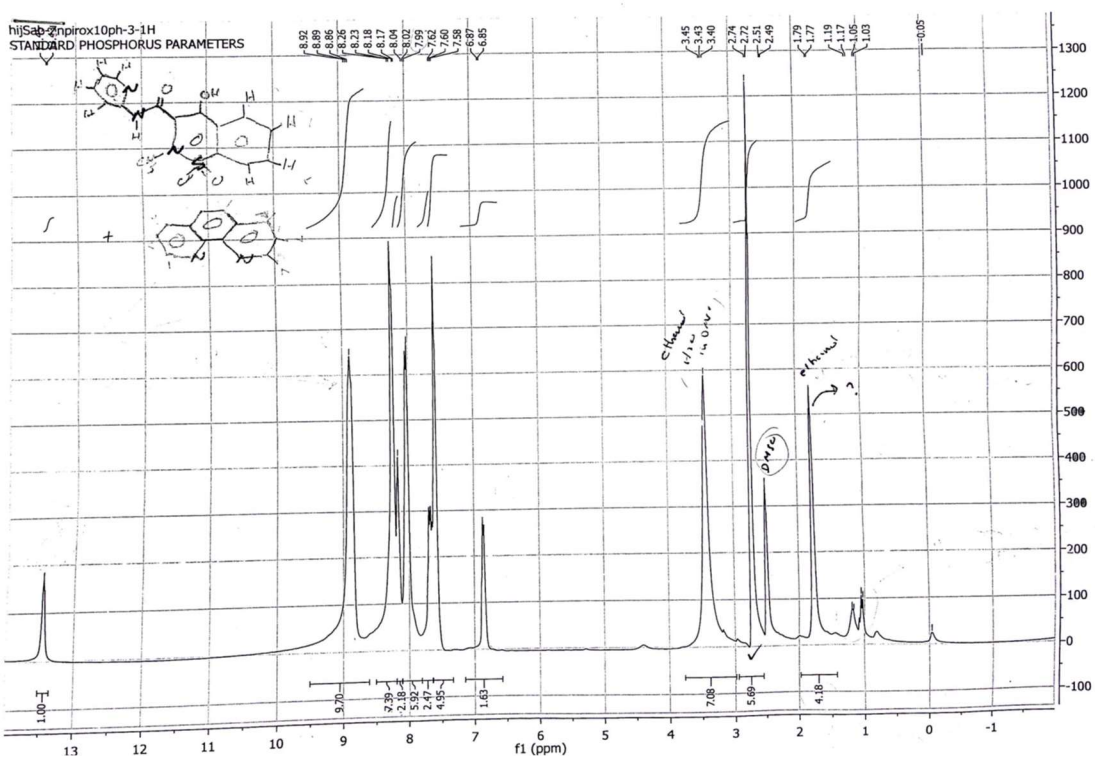

Figure S8: ^{1}H-NMR spectrum of complex **1.**

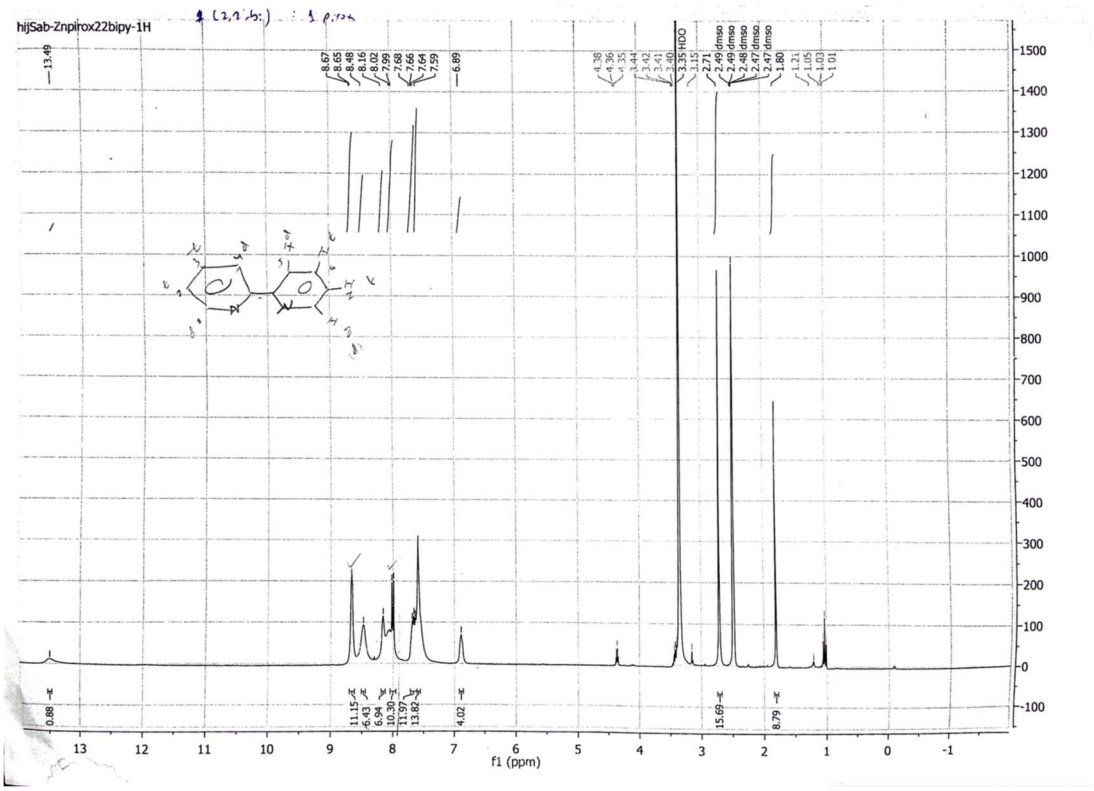

Figure S9: ^{1}H-NMR spectrum of complex **2.**

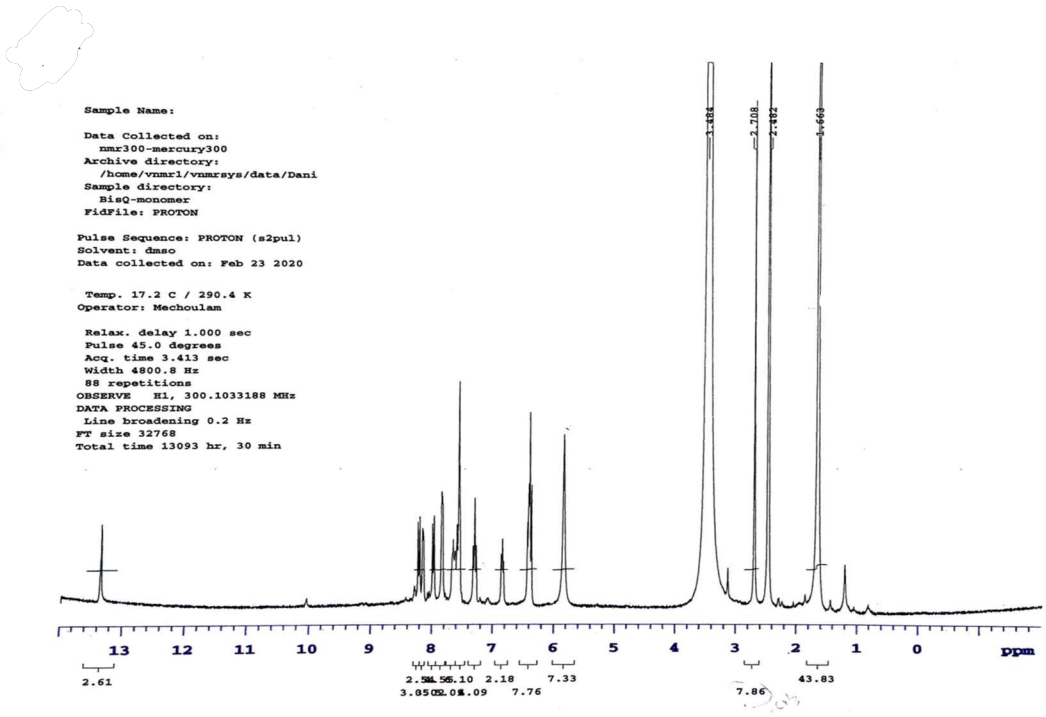

Figure S10: ^{1}H-NMR spectrum of complex **3**.

Table S1: ^{1}H-NMR spectral data of complexes **1**, Pir, and 1,10-phen, δ (ppm).

Complex **1**	Pir	1,10-phen
2.73 (s, 3H, CH_3)	2.78	
6.86 (d, 1H, CH, $^{3}J_{H\text{-}H}$ = 4.8 Hz)	6.53	
7.60 (m, 4H, 4CH)		7.56
8.03 (d, 4H, 4CH, $^{3}J_{H\text{-}H}$ = 6.9 Hz)	8.07	
8.18 (d, 4H, 4CH, $^{3}J_{H\text{-}H}$ = 3.0 Hz)		8.01
8.25 (d, 4H, 4CH, $^{3}J_{H\text{-}H}$ = 9 Hz)		8.45
8.88 (d, 4H, 4CH, $^{3}J_{H\text{-}H}$ = 6.0 Hz)		8.80
13.43 (s, 1H, NH)	10.75	
-(OH)	16.77	

Table S2: ^{1}H-NMR spectral data of complexes **2**, Pir, and 2,2'-biby, δ (ppm).

Complex **2**	Pir	2,2'-biby
2.71 (s, 3H, CH_3)	2.78	
6.89 (d, 1H, CH, $^{3}J_{H\text{-}H}$ = 6 Hz)	6.53	
7.59 (m, 3H, 3CH)	7.45	7.23
7.66 (m, 3H, 3CH)	7.61	7.74
8.0 (d, 1H, CH, $^{3}J_{H\text{-}H}$ = 9 Hz)	8.07	
8.48 (d, 1H, 2CH, $^{3}J_{H\text{-}H}$ = 3.6 Hz)	7.81	
8.66 (d, 2H, 2CH, $^{3}J_{H\text{-}H}$ = 3 Hz)		8.55
13.49 (s, 1H, NH)	10.75	
-(OH)	16.77	

Table S3: ^{1}H-NMR spectral data of complexes **3**, Pir, and 2-ampy, δ (ppm).

Complex **3**	Pir	2-ampy
2.71 (s, 3H, CH_3)	2.78	
5.85 (s, 4H, $2NH_2$)		7.40
6.40 (m, 3H, 3CH)	6.53	6.63
6.86 (t, 2H, 2CH, $^{3}J_{H\text{-}H}$ = 12 Hz)	6.62	6.73
7.30 (t, 1H, CH, $^{3}J_{H\text{-}H}$ = 7.2 Hz)	7.40	
7.63 (m, 3H, 3CH)	7.52	7.55
7.85 (d, 1H, CH, $^{3}J_{H\text{-}H}$ = 4.2 Hz)	7.81	
7.99 (d, 1H, CH, $^{3}J_{H\text{-}H}$ = 7.5 Hz)		8.04
8.16 (d, 1H, 1CH, $^{3}J_{H\text{-}H}$ = 3.9 Hz)	8.07	
13.39 (s, 1H, NH)	10.75	
- (OH)	16.77	

Table S4: ^{1}H-NMR spectral data of complexes **4**, Pir, and 2-picolyl, δ (ppm).

Complex **4**	Pir	2-picolyl
2.75 (s, 6H, $2CH_3$)	2.78	
4.02 (s, 4H, $2CH_2$)		4.57
6.88 (m, 4H, 4CH)	6.58	
7.26 (m, 4H, 4CH)		7.25
7.45 (dd, 2H, 2CH, $^{3}J_{H\text{-}H}$ = 6.5 Hz)	7.40	
7.51 (d, 2H, 2CH, $^{3}J_{H\text{-}H}$ = 7.8 Hz)		7.31
7.56 (d, 2H, 2CH, $^{3}J_{H\text{-}H}$ = 1.2 Hz)	6.53	
7.58 (d, 2H, 2CH, $^{3}J_{H\text{-}H}$ = 1.3 Hz)	7.50	
7.60 (d, 2H, 2CH, $^{3}J_{H\text{-}H}$ = 1.4 Hz)	7.66	
7.64 (m, 2H, 2CH)	7.55	
7.69 (m, 2H, 2CH)		7.74
7.78 (d, 2H, 2CH, $^{3}J_{H\text{-}H}$ = 1.7 Hz)	7.81	
8.27 (d, 2H, 2CH, $^{3}J_{H\text{-}H}$ = 8.4 Hz)	8.07	
8.48 (d, 2H, 2CH, $^{3}J_{H\text{-}H}$ = 4.8 Hz)		8.51
8.64 (t, 4H, $2NH_2$, $^{3}J_{H\text{-}H}$ = 4.8)		8.68
13.42 (s, 2H, 2NH)	10.75	
-(OH)	16.77	

Appendix D: *In-vitro* anti-bacterial activity data

Table S5: *In-vitro* anti-bacterial activity data for complexes (**1**-**4**) and their parent ligands against Gram-positive bacteria.

Compound	**Inhibition Zone Diameter (mm) ± standard deviation***				
	S. aureus	*M. luteus*	*B. subtilis*	*E. faecalis*	*S. epidermidis*
Erythromycin	39.5 ± 0.6	39.3 ± 0.6	32.5 ± 1.5	-	41.0 ± 1.0
Gentamycin	34.7 ± 1.2	37.7 ± 0.6	27.0 ± 2.0	-	36.7 ± 2.1
$Zn(CH_3CO_2)_2$	22.3 ± 2.1	-	13.7 ± 3.0	-	15.0 ± 0.0
Piroxicam	20.3 ± 0.6	-	-	-	26.7 ± 0.6
DMSO	-	-	-	-	-
1,10-phen.	29.3 ± 0.6	35.7 ± 1.2	30.3 ± 0.6	18.0 ± 1.0	34.3 ± 0.6
Complex **(1)**	23.7 ± 0.6	25.0 ± 0.0	20.3 ± 0.6	-	24.7 ± 0.6
2,2'-bipy	18.0 ± 0.0	26.0 ± 1.7	17.3 ± 0.6	-	25.0 ± 1.0
Complex **(2)**	13.6 ± 2.1	-	17.0 ± 0.0	-	24.3 ± 0.6
2-ampy	-	-	-	-	-
Complex **(3)**	12.7 ± 1.5	-	15.3 ± 0.6	-	22.7 ± 1.5
2-picolyl	19.3 ± 0.6	-	12.0 ± 0.0	-	14.0 ± 2.0
Complex **(4)**	22.0 ± 2.0	-	-	-	25.3 ± 0.6

*: The data in the table are average values of three experiments.

Table S6: *In-vitro* anti-bacterial activity data for complexes (**1**-**4**) and their parent ligands against Gram-negative bacteria.

Compound	**Inhibition Zone Diameter ± standard deviation (mm)***			
	P. aeruginosa	*K. pneumonia*	*P. mirabilis*	*E. coli*
Erythromycin	21.0 ± 2.6	19.7 ± 0.6	16.3 ± 0.6	19.7 ± 0. 6
Gentamycin	25.7 ± 1.2	24.7 ± 0.6	27.0 ± 2.0	22.3 ± 1.2
$Zn(CH_3CO_2)_2$	-	-	-	-
Piroxicam	-	-	-	-
DMSO	-	-	-	-
1,10-phen.	10.0 ± 0.0	28.3 ± 1.5	35.0 ± 0.0	28.7 ± 2.3
Complex **(1)**	-	20.7 ± 0.6	30.3 ± 1.2	20.0 ± 0.0
2,2'-bipy	-	23.7 ± 1.5	29.0 ± 0.0	22.3 ± 2.5
Complex **(2)**	-	9.3 ± 1.5	19.0 ± 0.0	10.3 ± 1.2
2-ampy	-	-	-	-
Complex **(3)**	-	-	-	-
2-picolyl	-	-	-	-
Complex **(4)**	-	-	-	-

*: The data in the table are average values of three experiments.